Southeastern Geology: Volume 49, No. 2 October 2012

Editor in Chief: S. Duncan Heron, Jr.

Abstract

Academic journal published quarterly by the Department of Geology, Duke University.

SOUTHEASTERN GEOLOGY

PUBLISHED

at

UNIVERSITY OF WEST GEORGIA

Duncan Heron

Editor-in-Chief

David M. Bush

Editor

This journal publishes the results of original research on all phases of geology, geophysics, geochemistry and environmental geology as related to the Southeast. Send manuscripts to **David Bush, Department of Geosciences, University of West Georgia, Carrollton, Georgia 30118, for Fed-X, etc. 1601 Maple St.,** Phone: 678-839-4057, Fax: 678-839-4071, Email: dbush@westga.edu. Please observe the following:

1) Type the manuscript with double space lines and submit in duplicate, or submit as an Acrobat file attached to an email.
2) Cite references and prepare bibliographic lists in accordance with the method found within the pages of this journal. Data citations examples can be found at http://www.geoinfo.org/TFGeosciData.htm
3) Submit line drawings and complex tables reduced to final publication size (no bigger than 8 x 5 3/8 inches, table text 8 pt Arial font).
4) Make certain that all photographs are sharp, clear, and of good contrast. Submit as jpeg quality 10 and pixel dimension at least 1600 for a landscape image.
5) Stratigraphic terminology should abide by the North American Stratigraphic Code (American Association Petroleum Geologists Bulletin, v. 67, p. 841-875).
6) Email Acrobat (pdf) submissions are encouraged.

Subscriptions to *Southeastern Geology* for volume 49 are: individuals - $28.00 (paid by personal check); corporations and libraries - $47.00; foreign $65. Inquiries should be sent to: **SOUTHEASTERN GEOLOGY, UNIVERSITY OF WEST GEORGIA, DEPARTMENT OF GEOSCIENCES, 1601 MAPLE STREET, CARROLLTON, GA 30118-0001**. Make checks payable to: *Southeastern Geology*.

Information about **SOUTHEASTERN GEOLOGY** is on the World Wide Web including a searchable author-title index 1958-2010 (Acrobat format). The URL for the Web site is: http://www.southeasterngeology.org

SOUTHEASTERN GEOLOGY is a peer review journal.

ISSN 0038-3678

SOUTHEASTERN GEOLOGY

Table of Contents

Volume 49, No. 2, October 2012

SOUTHEASTERN GEOLOGY
V. 49, No. 2, October 2012, p.49-97

PETROGENESIS OF GABBROIC CUMULATES AND INTRUSIVES OF THE CAROLINA SUPERTERRANE IN GEORGIA, SOUTHERN APPALACHIANS

JEFF B. CHAUMBA* AND MICHAEL F. RODEN

Department of Geology, University of Georgia, Athens, GA 30602
** Present address: Department of Geology & Geography*
210 Petrie Hall, Auburn University, Auburn, AL 36849, USA
Email: chaumba@auburn.edu

ABSTRACT

Rocks types of the Russell Lake Allochthon (RLA) in the Piedmont Province of the southern Appalachians in east central Georgia mapped by Allard and Whitney (1994, 1995) are metatroctolites, metaharzburgites, metagabbronorites, and meta-olivine gabbronorites. Some rocks display relict cumulate textures such as pseudomorphs after cumulate olivine and plagioclase and cumulate layering.

Bulk-rock geochemistry of RLA rocks displays a wide range in concentrations of oxides like MgO (~6 - 35 wt.%) and SiO_2 (~ 40 - 57 wt.%). This wide range of compositions appears to reflect igneous compositions of cumulate gabbros and ultramafic rocks as well as intrusive gabbros: for example, K_2O is inversely correlated with MgO, and CaO shows complex variations consistent with plagioclase control. Compatible trace elements such as Ni and Cr show high concentrations of over 800 ppm and 2000 ppm, respectively, in rocks with >25 wt.% MgO contents (such as olivine metagabbronorites and metaharzburgites) whereas in rocks with MgO contents of <10 wt.% MgO (such as metagabbronorites) the concentrations of both elements are below 200 ppm. Incompatible trace elements such as Rb are characterized by concentrations of over 25 ppm in rocks with <15 wt.% MgO, but drop to <10 ppm Rb in rocks with > 20 wt% MgO. Consequently, trace elements vary in a manner consistent with cumulate gabbroic rocks and metaharzburgites and intrusive gabbros.

Spidergrams of metagabbroic samples that show negative Nb depletions together with trace element discrimination diagrams point to formation of RLA samples at island arc settings. RLA rock samples investigated display a wide range in MgO contents such metaharzburgites, metatroctolites, and metagabbroic rocks, which further support their origin in an island arc setting. Such island arc crustal segments probably existed in the Iapetan Realm, and were later thrusted onto surrounding rocks during the final stages of the formation of Pangea due to collision between Laurentia and Gondwana.

INTRODUCTION

The southern and central Appalachian mountain belt extends from New York to Alabama (e.g., Hatcher, 2005; Hatcher and others, 2007). Rifting of the supercontinent Rodinia followed by collision between Laurentia and Gondwana occurred in at least 3 diachronous orogenic events in the Paleozoic {a) Ordovician-Silurian Taconic, b) Devonian Acadian and Devonian-Mississippian Neoacadian, and c) Pennsylvanian-Permian Alleghanian orogenies} resulted in the formation of the Appalachians (e.g., Hatcher, 2005; Hatcher and others, 2007).

Two belts of metamorphosed mafic/ultramafic rocks occur in the southern Appalachians: a "well-defined" belt outcropping in the western Blue Ridge, and an "ill-defined" belt poorly exposed in the Piedmont (Misra and Keller, 1978). In the southern Appalachians, most metamorphosed mafic/ultramafic bodies are highly altered compared to those from the northern Appalachians (Misra and Keller, 1978; Malpas, 1978). Most relatively large exposures of ultramafic bodies (predominantly metamorphosed dunites and peridotites) in the southern

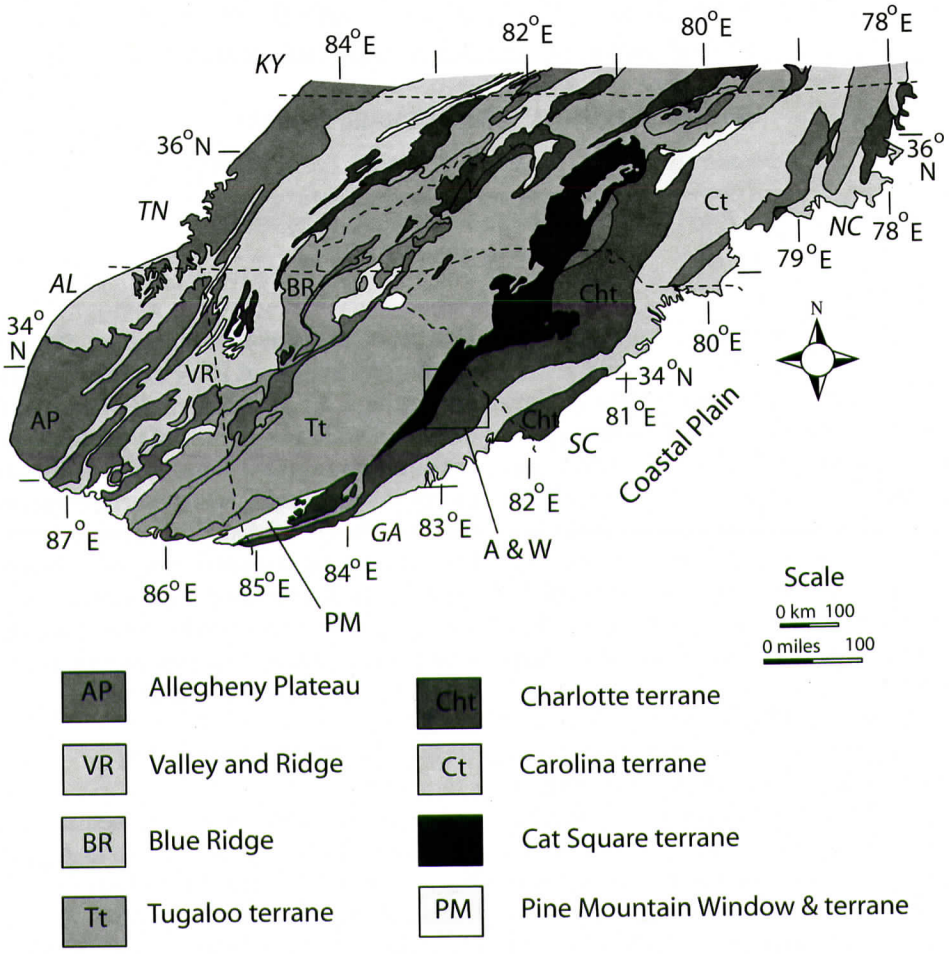

Figure 1. Simplified tectonic map of the southern Appalachians showing the different tectonic units (after Hatcher and others, 2007). Location of the area mapped by Allard and Whitney (1994) (A & W) is also shown.

Appalachians occur in the Blue Ridge Province. These Blue Ridge bodies are metamorphosed under amphibolite facies conditions (e.g., Misra and Keller, 1978; Swanson and others, 2005).

In addition, southern Appalachian metamorphosed mafic/ultramafic rocks in east central Georgia occur as relatively small bodies in the Carolina superterrane (Allard and Whitney, 1994). Allard and Whitney (1994) hypothesized that these bodies represent fragments of a thrust sheet emplaced over the Heardmont complex of gneisses of the Carolina superterrane (Legato, 1986; McFarland, 1992; Whitney and others, 1987; Allard and Whitney, 1994, 1995) during the Alleghanian deformation (Secor and others, 1986). Furthermore, Allard and Whitney (1994, 1995) hypothesized that the mafic/ultramafic bodies exposed in the Piedmont of Georgia represent "a layered dunite-to-gabbro body similar to oceanic crust" and coined the name, Russell Lake Allochthon (RLA) for these rocks. The thrust sheet model for the RLA was supported by work of Clippard and Hawman (1995) who interpreted shallow seismic reflection profiles on one of the meta-ultramafic bodies in northeast Georgia to indicate that the meta-ultramafic body had a shallow, sub-horizontal contact with the underlying gneisses.

An ophiolite has recently been defined, for example, by Dilek and Furnes (2011) as an al-

lochthonous fragment of upper-mantle and oceanic crustal rocks that is tectonically displaced from its primary igneous origin of formation due to plate convergence. Such a fragment should include a suite of, from bottom to top, peridotites and ultramafic to felsic crustal intrusive and volcanic rocks (with or without sheeted dikes) that can be geochronologically and petrogenetically related. In an incomplete ophiolite, some of these units may be missing. Emplacement of an ophiolite starts with displacement of oceanic lithosphere from its primary geodynamic environment and ends with its incorporation into mountain belts during orogenesis (Dilek and Furnes, 2011). Pelagic (chert or limestone) and/or Fe-Mn–rich hydrothermal sedimentary rocks stratigraphically overlie some ophiolites, whereas greenschist-amphibolite facies rocks related to tectonic displacement and emplacement also underlie other ophiolites (Dilek and Furnes, 2011). Kusky and others (2011) listed features or indicators that can be used in support of deformed or incomplete ophiolite sequences as convincing, supportive, diagnostic, distinctive, or typical. The occurrence of cumulates, for example, is supportive but not distinctive but the presence of layered gabbros is typical and supportive of an ophiolite in dismembered ophiolite sequences (Kusky and others, 2011). The occurrence of a basal thrust is sometimes considered necessary and supportive, although not diagnostic, of ophiolite sequences (Kusky and others, 2011).

Hatcher and others (2007) recently published a new tectonic map of the central and southern Appalachians (Fig. 1), which will be used to provide context in this investigation. This map is a compilation based on recent mapping and geochronologic data. Revised and new boundaries have emerged from this work, as well as a new terrane – the Cat Square terrane – as shown in Fig. 1 (Hatcher and others, 2007). Note that the other boundaries shown in Fig. 1 reflect this work, e.g., the Tugaloo terrane that straddles the Brevard zone in the southern Appalachians, indicates that the Brevard zone is not a suture (Hatcher and others, 2007). A second important interpretation is that the Charlotte and Carolina terranes form the composite Carolina superterrane, which is inferred to extend beneath Coastal Plain sediments to the East Coast magnetic anomaly (Hatcher and others, 2007). The RLA bodies are part of the eastern belt of metamorphosed mafic/ultramafic bodies in the southern Appalachians and occur in the Carolina superterrane (Hatcher and others, 2007).

This investigation focuses on the origin of metamorphosed mafic/ultramafic rocks exposed in the Piedmont of eastern and central Georgia that comprise the RLA of Allard and Whitney (1994, 1995). The purpose of our investigation was to build on the work of Allard and Whitney (1994) by clarifying the nature of the contact between the RLA and its country rocks based on field observations and detailed mapping of critical outcrops, and to test the "ocean crust" petrogenesis model of Allard and Whitney (1994) using new major and trace element analyses.

GEOLOGIC SETTING

The southern Appalachians extend from the New York promontory, located near the center and at the narrowest part of the orogen, to Alabama in the south (e.g., Hibbard and others 2006). Using lithotectonic divisions, Hibbard and others (2006) subdivided the entire Appalachian orogen into of three realms, Laurentian, Iapetan, and peri-Gondwanan. Based on this subdivision, the RLA is located within the Piedmont, which forms part of the Iapetan Realm. Domains were used at the scale of two or less embayments, and terranes are subdivisions of domains at the local scale using the Hibbard and others (2006) subdivisions. The Laurentian Realm encompasses rocks deposited either on or immediately adjacent to Laurentia, although structural windows of Laurentian rocks occur locally among some easterly accreted terranes (Hibbard and others 2006). Peri-Gondwanan Realm rocks occurring along the southeastern flank of the orogen formed proximal to Gondwana and they are therefore exotic with respect to Laurentian rocks. The Iapetan Realm is comprised of rocks of oceanic and volcanic arc affinity that have been caught between the

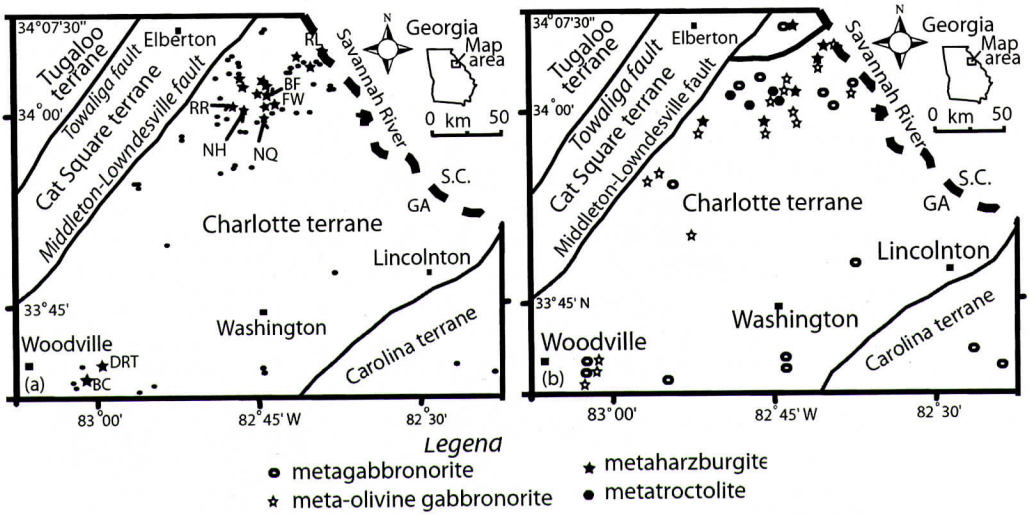

Figure 2. (a) Map showing the distribution of metamorphosed mafic and ultramafic bodies of the RLA (modified after Allard and Whitney, 1994). Abbreviations RR – River Road, NH – Nancy Hart complex, NQ - Norman Quarry, FW – Flatwoods, BF – Bakers Ferry, RL – Russell Lake, BC - Bethesda Church, and DRT – Durhamtown are bodies mentioned in the text. (b) Distribution of rock types in the area originally mapped as the RLA by Allard and Whitney (1994). Note the concentration of metaultramafic rocks in the northwestern/northern part of the Carolina superterrane.

Laurentian and peri-Gondwanan realms during the Appalachian orogeny (e.g., Hibbard and others, 2006).

PREVIOUS WORK ON MAFIC/ ULTRAMAFIC ROCKS OF THE SOUTHERN APPALACHIANS

In the Appalachians, Hess (1955) noted the occurrence of widespread mafic/ultramafic rocks. The majority of recent workers in the southern Appalachians have supported the interpretation of mafic/ultramafic bodies as dismembered ophiolites (Stoddard and others, 1982; Kite and Stoddard, 1984; Lipin, 1984; Stanley and others, 1984; Tenthorey and others, 1996; Berger and others, 2001; Swanson, 2001; Warner, 2001; Raymond and others, 2003). Some workers such as Hooper and Hatcher (1989) suggested that metamorphism, deformation, and alteration of some mafic/ultramafic rocks in the Carolina superterrane resulted from post-emplacement deformation of island arc-related rocks (Hooper and Hatcher, 1989).

The few available ages for these mafic/ultramafic bodies range from 410 ± 7 Ma (Acadian) based on U-Pb analyses of zircons from quartz diorite of the Union ultramafic complex in Maine in the northern Appalachians (Gaudette, 1981), to 490 ±20 Ma (Penobscottian) obtained from analyses of plagioclase, pyroxene, and whole-rock samples from the Baltimore Mafic Complex (Shaw and Wasserburg, 1984). The latter age is older than the typical southern Appalachian intrusive gabbro crystallization ages of 399 ± 27 to 407 ± 36 Ma (Acadian), also determined from plagioclase and clinopyroxene mineral separates and whole-rock samples, reported by McSween and others (1984), although one quartz-bearing gabbro yielded an age of 479 ± 24 Ma (McSween and others, 1984).

Shaw and Wasserburg (1984) reported whole-rock ε_{Nd} (at 490 Ma) values of -2.2 to -6.4 and initial $^{87}Sr/^{86}Sr$ ratios between 0.7075 and 0.7120 for the Baltimore Mafic Complex. Based on these enriched Nd and Sr isotope signatures, the Baltimore Mafic Complex was interpreted as a subduction-related continental intrusion, which was contaminated by old con-

tinental crust at the time of intrusion.

FIELD RELATIONSHIPS AND PETROGRAPHY

A detailed map of the distribution of the RLA and its country rocks was provided by Allard and Whitney (1994); we focused on further evaluation of the nature of the contact between the metamorphosed mafic/ultramafic RLA bodies and the underlying country rocks as well as examining and documenting lithologies and relict igneous textures. The locations of some key bodies that were sampled and in some cases mapped are shown in Fig. 2a (note that these bodies are informally named after local landmarks). Other samples, however, were from exposures that are too small (< $1m^2$) to show on maps.

The contact between the RLA bodies and the local country rocks is generally poorly exposed (Allard and Whitney, 1994). However at the RLA type locality, the Russell Lake body (Fig. 2a), Whitney and Allard (1994) described sheared basal rocks of the RLA in contact with metadacites of the Carolina superterrane (Fig. 3). Through trenching, we documented similar, shallow and subhorizontal contacts at the Flatwoods and Durhamtown bodies although no shearing was observed at the contacts.

Metamorphosed mafic/ultramafic rocks from the study area have been classified, on the basis of their petrography, texture, and normative mineralogy into metamafic rocks (meta-olivine gabbronorites, metagabbronorites, and metatroctolites) and meta-ultramafic rocks (metaharzburgites), (e.g., Fig. 2b). Typically a complex mixture of chlorite, serpentine, zoned amphibole (core of pargasite or magnesiohornblende rimmed by tremolite/actinolite), and epidote has replaced the original iron-magnesium silicates and plagioclase. Only rarely are remnants of calcic plagioclase, olivine, and clinopyroxene found, and no remnant orthopyroxene crystals were observed.

Due to the interpretation that most of the original iron-magnesium silicates have almost all been completely metamorphosed to amphibole, chlorite, serpentine, and talc, distinction of the rock types into meta-orthopyroxenites, metaharzburgites, metaclinopyroxenites, and metawebsterites, which is dependent on the presence and abundances of these minerals, is no longer possible from mineralogy. Consequently we adopted a strategy of calculating normative mineralogy, and then using the normative mineralogy to name rocks following the International Union of Geological Sciences (IUGS) classification system (Streckeisen, 1976). Implicit in this approach to name rocks is the assumption of closed system metamorphism (excluding water); we justify this approach in a later section.

Relict layered textures were observed at some RLA localities. For example in the Norman Quarry body relict layering was observed. The layers are defined by relative amounts of plagioclase and amphibole but originally the layers were probably defined by relative amounts of plagioclase and an anhydrous ferromagnesian silicate. Hand sample textures are also indicative of the very coarse-grained nature of some RLA rocks: for example, in a sample from Norman Quarry body where plagioclase, interpreted to be intercumulus material, partially encloses amphibole grains (interpreted to be pseudomorphs after anhydrous ferromagnesian silicates) (Fig. 4).

Metagabbronorites and olivine metagabbronorites are the predominant rock types, with few metatroctolites and even fewer metaharzburgites (Fig. 5). The mineralogy of the metagabbronorites is zoned amphibole, plagioclase (zoned with calcium-rich core and a very thin sodium-rich rim), epidote, quartz, zoisite/clinozoisite, and opaque minerals (Fig. 6). The hornblende cores of the zoned amphiboles are typically dark green, and a thin light green rim of actinolite/tremolite commonly surrounds the cores. Rare metagabbroic exposures, such as those outcropping at Durhamtown, are typically very coarse-grained (1-2 cm) and they also contain clinopyroxene. Amphiboles are typically coarse-grained, up to 2cm in size, whereas other minerals like zoisite/clinozoisite are typically fine-grained with grains less than 1mm in size. Plagioclase crystals from the Durhamtown body typically range in size from 1-5mm. The

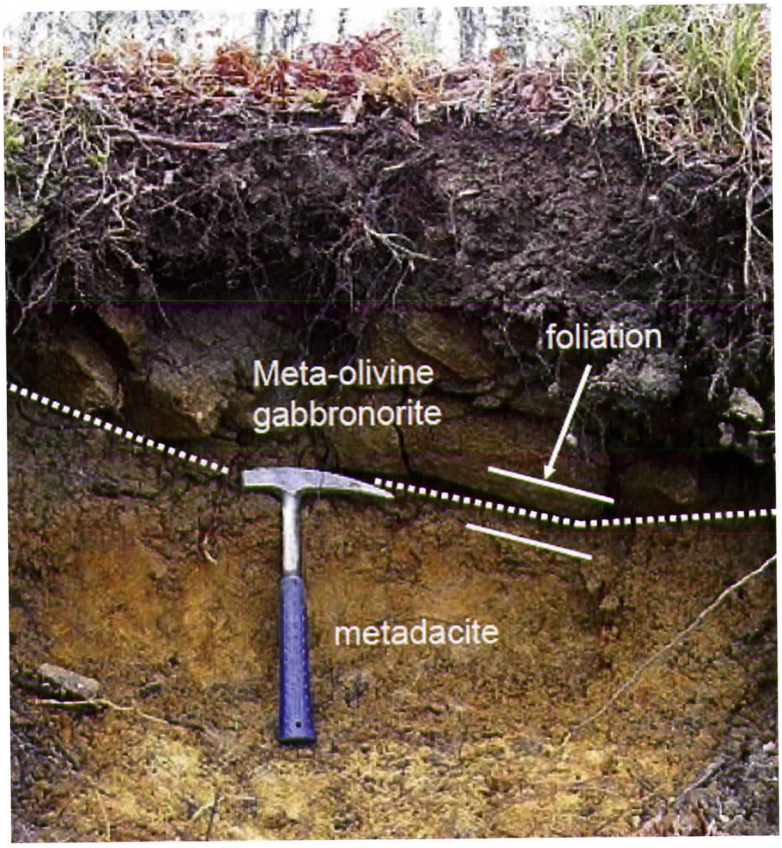

Figure 3. Photograph showing horizontal foliation displayed by the mafic rocks of the RLA at its type locality overlying sheared metadacitic country rocks. Location is on the western shore of Russell Lake north of US Highway 72, Heardmont quadrangle, eastern Georgia (Legato, 1986). White lines in photo represent trends of foliation.

Figure 4. Left: Photograph of hand specimen showing relict intercumulus plagioclase partially enclosing amphibole (inferred to be initially pyroxene from norm compositions). Pencil is 18.5 cm long. Norman Quarry, Jackson Crossroads Quadrangle. Right: Hand specimen of metawehrlite showing chlorite and serpentine crystals (greenish in color) and amphibole (brownish and light colored). Lighter patches are inferred to be former cumulate olivine crystal in a matrix of former clinopyroxene based on norm compositions. Sample 3-10MW, Bakers Ferry body, Elberton East Quadrangle.

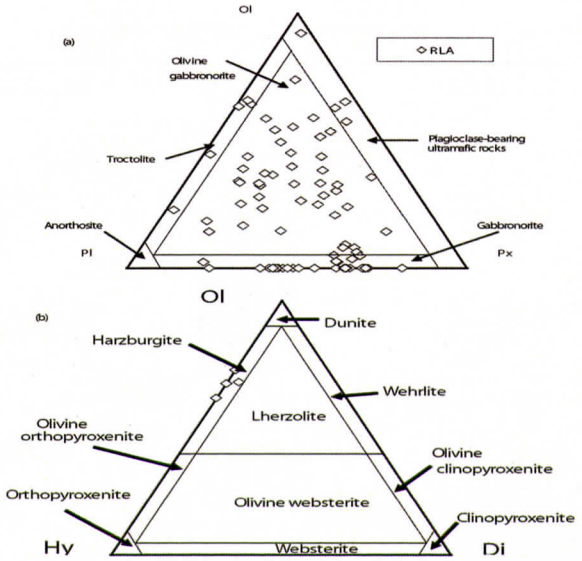

Figure 5. Plot showing normative compositions from the RLA plotted on IUGS classification diagrams. (a) Plot of Olivine (Ol), plagioclase (Pl), and pyroxene (Px) showing that the bulk of RLA rocks are metapyroxenites and metagabbros with very few ultramafics. (b) Plot of the few ultramafic rocks from the RLA on an Ol, hypersthene (Hy), and diopside (Di) plot showing that the few ultramafic rocks from the RLA are metaharzburgites.

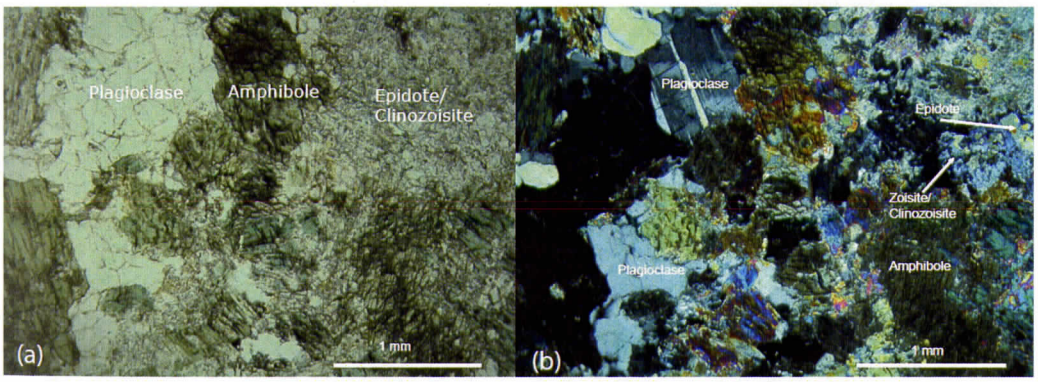

Figure 6. Metagabbronorite from Durhamtown metamafic complex consisting of plagioclase, zoned amphibole, and epidote/clinozoisite. Sample 17-3SS3: (a) - Plane polarized light, (b) - Cross polarized light.

other minerals range in grain size from fine- to coarse-grained. Clinopyroxene is coarse-grained, and is colorless to pale green under plane polarized light. Plagioclase appears unzoned when seen under the microscope, but zoning is occasionally observed on backscattered electron images.

Olivine metagabbronorites have almost comparable mineralogy to the metagabbronorites, and the minerals range in size from fine (~0.5mm) to coarse-grained (mostly over 1cm in size). The only noticeable difference between olivine metagabbronorites and metagabbronorites is an increased modal abundance of amphiboles accompanied by a decreased modal abundance of plagioclase. Some samples have very little modal plagioclase whereas others are characterized by abundant plagioclase which

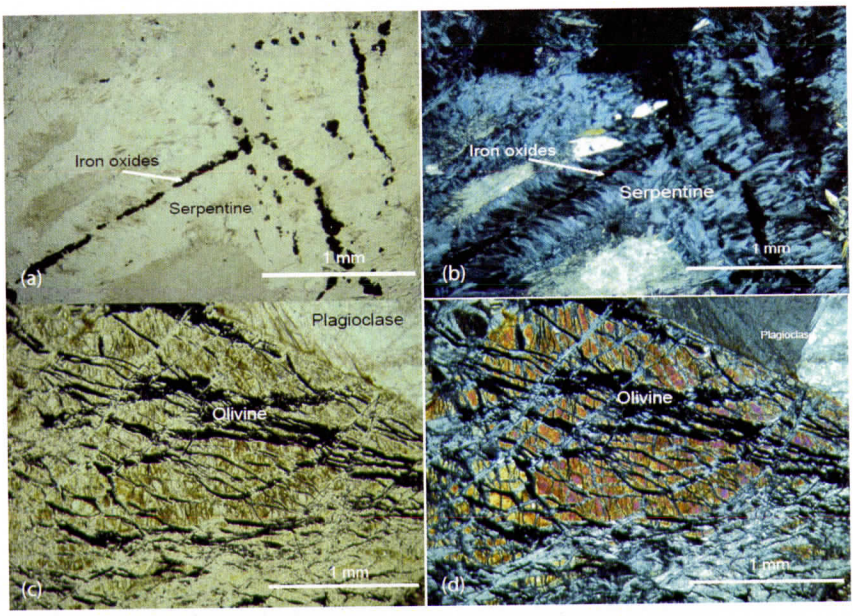

Fig 7. Metatroctolite from Dr George Ward Drive showing original olivine crystal shapes outlined by iron oxides in a coarse-grained metatroctolite. The olivine is now almost completely altered to serpentine. Sample GW2: Elberton East Quadrangle, (a) - Plane polarized light, (b) - Cross polarized light; Metatroctolite from River Road body; sample RRN, Jackson Crossroads Quadrangle, (c) - Plane polarized light, (d) - Cross polarized light.

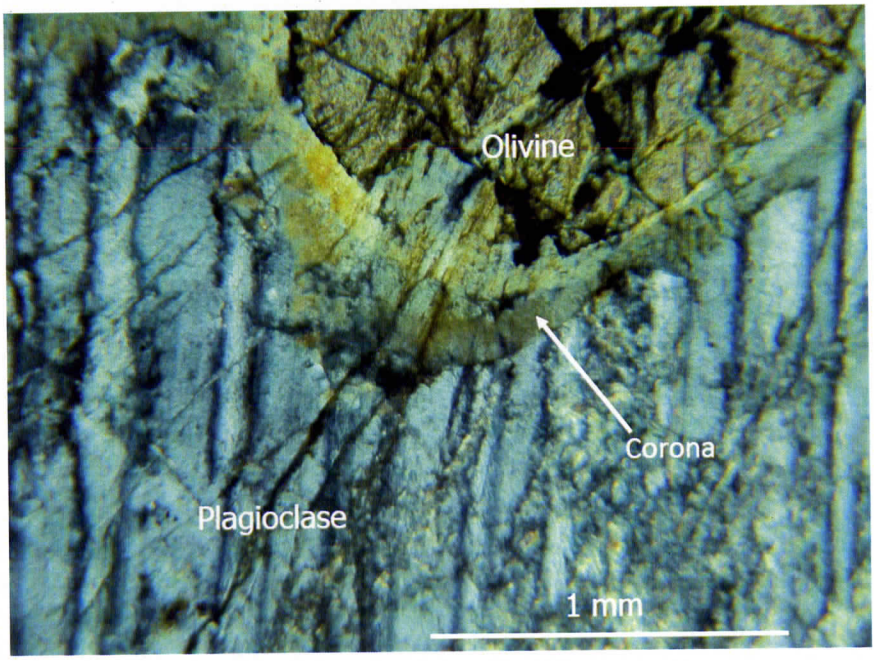

Figure 8. Metatroctolite from Bakers Ferry body showing orthopyroxene, hornblende and hornblende/spinel symplectite corona texture between olivine and plagioclase. Sample 3-10a: Elberton East Quadrangle, Cross polarized light.

can reach up to 40% of the mode. Zoned amphiboles similar to those that occur in metagabbronorites are common in olivine metagabbronorites.

Exposures of metatroctolites occur along Bakers Ferry and Elam Roads in the Elberton East quadrangle. Additional exposures of metatroctolites occur in Jackson Crossroads quadrangle along River Road to the west of Georgia State Route 17. Most metatroctolites exposures are very coarse-grained, with both olivine and plagioclase grain sizes typically exceeding 3mm in size. In places, metatroctolites are composed of very coarse-grained relict olivine crystals that retain original crystal shapes and textures. Metatroctolites are highly dissected by veins and veinlets of iron oxides occurring together with euhedral and zoned medium- to coarse-grained plagioclase crystals. Fig.7 shows well-developed relict olivine crystal shapes defined by opaque oxides.

Where olivine is in contact with plagioclase as is the case in metatroctolites, coronas are common as shown in Fig. 8. The coronas are composed of an orthopyroxene shell that partially rims the olivine, and the orthopyroxene is in turn rimmed by hornblende. Surrounding the hornblende are spinel-hornblende symplectites which are in contact with plagioclase. Spinel, which is light green under plane-polarized light, is also present as relatively large, discrete grains in some corona-bearing metatroctolites.

Metaharzburgite outcrops are few and they are restricted to the northern half of the area originally mapped by Allard and Whitney (1994). Metaharzburgites are composed of amphiboles (pargasites), in some samples the serpentine is inferred to be replacing former olivine grains. Plagioclase is rare in metaharzburgites, and only occurs as a few anhedral grains interpreted to be intercumulus. Grain sizes of the amphibole crystals in metaharzburgites range from medium- to coarse-grained (averaging ~3mm in size).

ANALYTICAL METHODS

Representative samples of different rock types and outcrops of the investigated area were selected for bulk-rock analyses following examination of thin sections. A total of 55 samples were first crushed in a hardened steel jaw-crusher to produce chips smaller than 1 cm in size. A quarter of the jaw-crushed chips obtained by cone-and-quartering were ground in a hardened steel shatterbox to produce approximately 40g of rock powder.

Approximately 10.0 g of the rock powder were weighed and mixed with 2 ml of acetone/elvacite solution to produce powder pellets through applying a pressure of 21, 000 kPa. Trace element analyses were then made on the pressed powder pellets at the University of Georgia Center for Applied Isotope Studies on a Philips 2.4 kW Magix x-ray fluorescence spectrometer. The instrument is equipped with an Rh anode and a sequential spectrometer and the power settings varied according to the element of interest. Data obtained were corrected for peak overlaps and mass absorption effects. The analytical lines used were Kα with the exception of Ba, Hf, U, and Th, for which the Lα analytical line was used.

Major element analyses were carried out on fused glass disks following a slight modification of the method of Norrish and Hutton (1969). Approximately 10.00 g of lithium borate-lithium bromide fusion flux was weighed and added to approximately 2.50 g of sample to produce fused glass disks. The disks were analyzed utilizing the same instrument as was used for trace elements and data were corrected for peak overlap and mass absorption effects. Replicate analyses of USGS standards indicated precisions of ± 1% (1 S.D.) for most major and trace elements.

MAJOR OXIDE ABUNDANCES

Bulk-rock major element geochemical data from the RLA are presented in Table 2. Before any discussion of the bulk-rock geochemical data from the study area can be made, it is necessary to make an assessment of the suitability of the geochemical data for use in petrogenetic studies given the intense weathering rates in humid climatic environments such as those in the southeastern United States. In such climatic

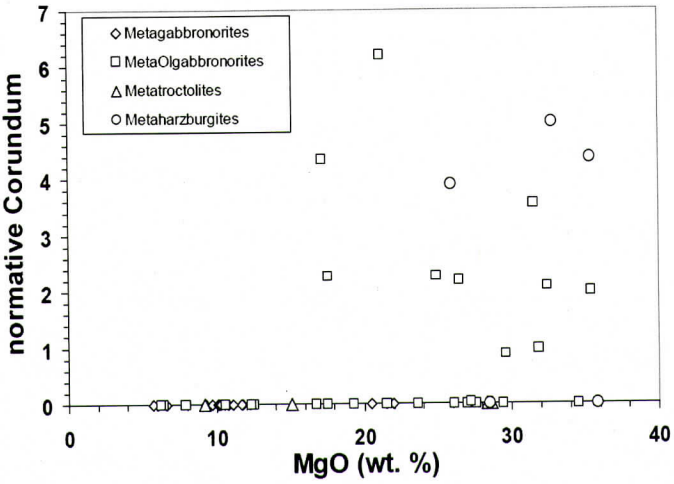

Figure 9. Plot of normative corundum (wt.%) *versus* MgO (wt.%) for samples from the study area. Eleven of the 55 RLA samples have normative corundum contents of over 1 wt.% and are considered unrepresentative of their original protoliths.

conditions, bulk-rock compositions of mafic/ultramafic rocks may be altered to an extent that they are no longer representative of the protoliths of the rocks (Chaumba and Swanson, 2008). This is reflected by samples with normative corundum contents higher than 1%.

Figure 9 is a plot of magnesium oxide *versus* normative corundum for rocks from the RLA. Unaltered mafic/ultramafic igneous rocks have no or negligible corundum in their CIPW norms (e.g., Best, 2003). Eleven of the 55 samples from the RLA plotted in Fig. 9 have normative corundum contents of over 1%, and these samples generally have high magnesium numbers (Mg# = 100 x Mg/(Mg + FeO)) of over 70 (Table 2). These 11 normative corundum-bearing samples are considered to have compositions which are not representative of their original igneous compositions, and to have suffered modification of their bulk compositions by weathering (Chaumba and Swanson, 2008); thus they are not further considered here. Inclusion of these samples, however, has no significant effect on the geochemical trends presented.

The nature of bulk rock compositions can best be assessed by using recalculated anhydrous compositions because some of the samples have high loss on ignition (LOI) values of > 5% (Table 2; e.g., McFarland, 1992; Owens and Uschner, 2001). LOI in the rocks under investigation is caused by hydrous minerals that are produced during metamorphism. Furthermore, in the case of similar rocks from the Piedmont of Virginia, Owens and Uschner (2001) stated that anhydrous compositions better approximate the compositions of the protoliths, and the use of anhydrous compositions resulted in no significant changes in the relative positions of the plotted data points. However, it should be borne in mind that mafic arc magmas can have liquidus H_2O concentrations ranging from >0.5 up to ~6.2 wt.% (e.g., Sisson and Layne, 1993) and 0.3-2.4 wt.% at active subduction zones (e.g., Walker and others, 2001).

In Fig. 10, major element oxides normalized to 100% anhydrous are plotted relative to MgO contents – the latter oxide varies widely between ~ 5 and 35 wt.% in the rocks of the RLA. Shown in Fig. 10a is a plot of silica versus magnesia. Silica contents also vary widely from a low of 40.4 wt.% in a metaharzburgite to a high value of 59.7 wt.% in a metagabbronorite. However, there is no good correlation between magnesia and silica. In contrast to SiO_2, Al_2O_3 and MgO display a negative correlation: MgO contents decrease as Al_2O_3 contents increase (Fig. 10b). Al_2O_3 contents ranging from approximately 3 to 26 wt.% are found in RLA

Table 1. Samples, lithologies, mineralogies, and GPS coordinates of representative RLA rocks.

Sample	Body	Rock Type	Mineralogy#	~Size (m^2)	X co-ordinate	Y co-ordinate
17-3N	DRT	Mg	Amp, Pl, Kfs, Cpx, Czo, Qz, Ep, Opq	40000	82°59.371'W	33°40.193'N
17-3NN	DRT	Mg	Amp, Pl, Kfs, Cpx, Czo, Qz, Ep, Opq	"	82°59.369'W	33°40.158'N
17-3SN	DRT	Mg	Amp, Pl, Kfs, Cpx, Czo, Qz, Ep	"	82°59.437'W	33°40.083'N
17-3SS1	DRT	Mog	Amp, Cpx, Czo, Ep	"	82°59.436'W	33°40.117'N
17-3SS2	DRT	Mog	Amp, Pl, Kfs, Cpx, Czo, Qz,	"	82°59.426'W	33°40.096'N
17-3SS3	DRT	Mg	Amp, Pl, Kfs, Cpx, Czo, Qz,	"	82°59.451'W	33°40.079'N
RC20	DRT	Mg	Amp, Pl, Kfs, Cpx, Czo, Qz, Ep, Opq	"	82°59.407'W	33°40.288'N
RC22	DRT	Mg	Amp, Pl, Kfs, Cpx, Czo, Qz,	"	82°59.420'W	33°40.094'N
RC23	DRT	Mg	Amp, Pl, Kfs, Cpx, Czo, Qz,	"	82°59.446'W	33°40.073'N
RC25	DRT	Mg	Amp, Pl, Kfs, Cpx, Czo, Qz,	"	82°59.468'W	33°40.022'N
DRTCMG	DRT	Mg	Amp, Pl, Kfs, Cpx, Czo, Qz, Ep	40000	82°59.417'W	34°40.162'N
8-2A	F[1]	Mh	Amp, Srp, Chl, Ep, Czo, Tlc, Opq	600000	82°44.141'W	33°59.779'N
8-2B	F	Mog	Amp, Chl, Czo,	"	82°44.178'W	33°59.729'N
8-4A	F	Mg	Amp, Qz	"	82°44.076'W	33°59.658'N
8-4B	F	Mog	Amp, Czo, Ep, Opq	"	82°44.077'W	33°59.661'N
8-4C	F	Mog	Amp, Opq, Ep	"	82°44.077'W	33°59.663'N
8-6A	F	Mog	Amp, Chl, Czo, Ep	"	82°43.877'W	33°59.740'N
8-6Ci	F	Mog	Amp, Chl, Czo, Ep	"	82°43.856'W	33°59.705'N
8-7D	F	Mg	Amp, Qz	"	82°43.781'W	34°00.024'N
BC1	BC	Mg	Amp, Pl, Kfs, Czo, Ep, Opq	50000	83°00.761'W	33°39.107'N
BC2	BC	Mg	Amp, Pl, Kfs, Czo, Ep, Opq	"	83°00.778'W	33°39.102'N
BC3	BC	Mg	Amp, Pl, Kfs, Czo, Ep, Kfs, Opq	"	83°00.801'W	33°39.108'N
BC4	BC	Mg	Amp, Pl, Kfs, Czo, Ep, Opq	"	83°00.824'W	33°39.092'N
BC5	BC	Mog	Amp, Pl, Kfs, Czo, Ep, Opq	"	83°00.834'W	33°39.078'N
BC6	BC	Mog	Amp, Pl, Kfs, Czo, Ep, Opq	"	83°00.845'W	33°39. 073'N
NQLPG	NQ	Mog	Amp, Pl, Kfs, Czo, Ep, Opq	2000	82°47.038'W	33°55.770'N
NQEPN	NQ	Mog	Amp, Pl, Kfs, Czo, Ep, Opq	"	82°47.029'W	33°55.774'N
NQNE	NQ	Mog	Amp, Pl, Kfs, Czo, Ep, Opq	"	82°47.010'W	33°55.782'N
3-10A	B.F.	Mog	Ol, Pl	10000	82°45.653'W	34°02.119'N
3-10G	B.F.	Mog	Amp, Tlc	"	82°45.692'W	34°02.116'N
3-10MW	B.F.	Mog	Amp, Ep, Czo, Opq	"	82°45.724'W	34°02.096'N
3-10NEC	B.F.	Mt	Amp, Pl, Ep, Czo	"	82°45.697'W	34°02.175N
3-10W	B.F.	Mog	Chl, Amp	"	82°45.894'W	34°02.101'N
Bell1	N.H.[2]	Mog	Chl, Amp, Tlc, Opq	20000	82°48.239'W	33°59.015'N
Bell2	N.H.	Mog	Ol, Chl, Srp, Opq	"	82°48.234'W	33°59.015'N
Bell3	N.H.	Mog	Ol, Chl, Srp, Amp, Opq	"	82°48.226'W	33°59.016'N
Bell4	N.H.	Mh	Amp, Chl, Tlc, Opq	"	82°48.206'W	33°59.010'N
BellN1	N.H.	Mog	Ol, Srp, Amp, Opq	"	82°48.211'W	33°59.034'N

Sample	Body	Rock Type	Mineralogy#	~Size (m^2)	X co-ordinate	Y co-ordinate
BellN2	N.H.	Mog	Amp, Chl, Opq	"	82°48.211'W	33°59.068'N
BellN3	N.H.	Mog	Amp, Pl, Opq	"	82°48.215'W	33°59.087'N
RRN	N.H.	Mh	Ol, Srp, Pl, Amp, Opq	20000	82°49.913'W	34°00.341'N
3-6	-	Mog	Amp, Opq	-	82°47.315'W	34°03.279'N
3-8i	NBF	Mog	Amp, Pl, Opq	1000	82°46.477'W	34°02.818'N
3-8ii	NBF	Mog	Tlc, Amp, Ep, Opq	1000	82°46.498'W	34°02.807'N
4-3	-	Mog	Amp, Chl, Opq	-	82°40.521'W	34°03.926'N
4-4	-	Mog	Amp, Srp, Opq	-	82°40.897'W	34°03.832'N
4-13	-	Mog	Amp, Ep	-	82°44.357'W	34°02.493'N
4-17	-	Mh	Srp, Chl, Amp, Opq	-	82°44.063'W	34°01.881'N
RLAe	R.L.	Mh	Amp, Tlc, Chl, Czo, Opq	100	82°38.934'W	34°04.005'N

Bodies: DRT – Durhamtown; BC – Bethesda Church; F – Flatwoods; NQ – Norman Quarry; B.F. – Bakers Ferry, NBF – North Bakers Ferry; N.H. – Nancy Hart complex. Rock types: Mg- metagabbronorites; Mog – meta-olivine gabbronorite; Mh – metaharzburgite, Mt – metatroctolite; * – based on normative compositions; [1] - comprised of at least 6 different bodies; [2] - comprised of at least 3 different bodies; # - Mineral abbreviations follow recommendation of Whitney and Evans (2010).

Table 2. Bulk-rock major element oxide abundances for RLA rocks.

Sample	Type	Mg#	SiO_2	TiO_2	Al_2O_3	$Fe_2O_3^t$	MnO	MgO	CaO	Na_2O	K_2O	P_2O_5	LOI[1]	Total
17-3N	Mg	57.8	54.43	0.46	10.77	8.16	0.16	10.06	13.97	1.25	1.00	0.09	0.71	100.07
17-3NN	Mg	57.2	51.67	0.48	9.44	9.75	0.29	11.72	14.61	1.03	0.37	0.11	0.48	99.95
17-3SN	Mg	62.4	56.47	0.40	8.61	7.04	0.17	10.50	14.32	1.16	0.66	0.07	1.04	100.43
17-3SS1	Mog	61.2	49.97	0.51	9.97	8.65	0.15	12.30	16.37	0.92	0.48	0.14	0.94	100.40
17-3SS2	Mog	61.8	52.49	0.58	10.77	9.34	0.17	9.48	14.11	1.18	0.92	0.28	0.72	100.04
17-3SS3	Mg	55.6	50.67	0.46	14.02	8.17	0.17	9.19	14.77	1.15	0.57	0.154	1.60	100.90
RC20	Mg	62.7	55.40	0.39	10.76	6.41	0.12	9.70	14.76	1.79	0.52	0.04	0.98	100.87
RC22	Mg	62.6	53.95	0.51	9.23	7.70	0.16	11.62	14.66	1.01	0.55	0.03	0.53	99.95
RC23	Mg	63.8	56.58	0.42	8.07	6.77	0.24	10.75	14.76	1.27	0.85	0.08	0.92	100.71
RC25	Mg	64.6	50.29	0.48	9.44	8.57	0.20	12.52	16.94	0.80	0.41	0.11	1.05	100.81
DRTCMG	Mg	43.8	56.86	0.50	13.54	8.74	0.14	5.46	9.15	1.38	0.25	0.05	5.08	101.14
8-2A	Mh	70.9	39.96	0.06	13.18	11.18	0.13	24.50	5.21	0.02	0.03	0.01	6.92	101.20
8-2B	Mog	70.6	41.33	0.06	15.82	9.07	0.13	19.63	9.70	0.01	0.10	0.01	5.53	101.39
8-4A	Mg	41.5	52.05	0.67	16.07	10.16	0.11	6.49	11.08	0.09	0.05	0.14	2.68	100.59
8-4B	Mog	69.1	41.84	0.08	18.59	8.33	0.13	16.78	8.31	0.24	0.89	0.01	6.13	101.32
8-4C	Mog	67.7	41.16	0.04	19.68	8.66	0.14	16.34	7.72	0.59	0.53	0.01	6.20	101.07
8-6A	Mog	66.2	42.91	0.07	12.81	11.72	0.18	20.64	7.03	0.37	0.06	0.01	5.15	100.94
8-6Ci	Mog	68.4	40.81	0.07	14.52	10.83	0.19	21.06	8.16	0.04	0.03	0.01	5.74	101.45
8-7D	Mg	34.9	49.94	0.67	17.10	11.96	0.17	5.77	8.66	0.88	0.06	0.04	5.44	100.69
BC1	Mg	59.5	53.30	0.44	11.14	7.59	0.16	10.03	14.47	1.22	0.98	0.10	1.07	100.50
BC2	Mg	55.2	50.55	0.60	11.37	9.10	0.18	10.09	15.30	1.21	0.50	0.20	0.53	99.63
BC3	Mg	60.9	54.78	0.42	9.93	7.31	0.14	10.23	14.52	1.40	0.73	0.13	0.46	100.05
BC4	Mg	61.5	51.56	0.47	9.82	7.72	0.15	11.08	16.69	1.19	0.61	0.14	0.54	99.96
BC5	Mog	61.1	50.12	0.50	10.13	8.60	0.17	12.18	16.05	1.00	0.41	0.16	0.45	99.76
BC6	Mog	57.1	50.83	0.55	11.33	8.74	0.16	10.49	14.92	1.33	0.69	0.18	1.12	100.34

NQLPG	Mog	66.7	43.23	0.10	15.15	9.46	0.14	17.04	11.42	0.36	0.07	0.01	3.49	100.46
NQEPN	Mog	65.1	42.98	0.11	14.90	9.66	0.14	16.24	12.18	0.43	0.08	0.01	4.01	100.74
NQNE	Mog	66.2	42.82	0.10	13.66	10.59	0.15	18.63	10.25	0.39	0.09	0.01	3.95	100.63
3-10A	Mog	70.9	39.47	0.02	11.64	13.27	0.17	25.92	6.28	0.37	0.04	0.01	4.40	101.59
3-10Bi	Mog	70.0	39.94	0.05	9.81	13.99	0.20	26.10	5.25	0.30	0.12	0.01	4.93	100.69
3-10Bii	Mt	70.8	38.88	0.02	10.36	13.81	0.19	26.88	5.72	0.25	0.05	0	4.72	100.88
3-10D	Mt	71.2	39.59	0.02	10.39	13.96	0.18	27.62	5.50	0.38	0.05	0	3.21	100.91
3-10E	Mog	61.2	34.81	0.03	17.64	15.58	0.21	19.71	6.49	0.01	0.04	0	4.91	99.43
3-10F	Mt	54.9	39.61	0.30	17.54	14.80	0.18	14.43	9.13	0.82	0.34	0.01	4.60	101.75
3-10G	Mog	65.7	38.73	0.02	11.8	15.14	0.17	23.18	5.28	0.03	0.03	0	6.60	100.99
3-10MW	Mog	33.5	39.17	1.23	16.10	18.97	0.17	7.65	13.95	0.69	0.22	0.01	2.21	100.38
3-10NEC	Mt	65.2	42.48	0.04	25.85	5.96	0.08	8.95	13.75	1.08	0.10	0.02	2.69	100.98
3-10W	Mog	76.1	42.49	0.02	10.93	10.04	0.12	25.64	5.83	0.02	0.03	0	6.60	101.73
Bell1	Mog	72.2	39.07	0.06	6.93	14.33	0.14	29.80	2.74	0.01	0.03	0	7.98	101.08
Bell2	Mog	70.4	37.91	0.05	4.51	16.84	0.22	32.01	2.62	0.02	0.03	0	7.23	101.44
Bell3	Mog	70.9	39.83	0.04	7.51	15.01	0.14	29.27	2.27	0.03	0.03	0	7.05	101.19
Bell4	Mh	70.8	38.05	0.05	4.95	16.63	0.15	32.26	0.53	0	0.02	0	8.02	100.66
BellN1	Mog	72.0	40.78	0.06	9.71	12.07	0.17	24.84	8.44	0.26	0.05	0	5.56	101.94
BellN2	Mog	70.4	40.66	0.06	9.74	12.08	0.17	24.67	8.44	0.24	0.05	0	5.17	101.28
BellN3	Mog	34.4	45.58	1.84	16.04	14.94	0.18	6.27	11.86	2.31	0.10	0.11	0.86	100.09
RRN	Mh	68.0	37.65	0.03	9.18	15.60	0.20	26.58	5.17	0.22	0.04	0	6.17	100.84
3-6	Mog	72.8	45.47	0.67	9.78	10.51	0.12	22.49	6.36	0.48	0.08	0.12	5.00	101.09
3-8i	Mog	39.7	46.56	1.28	19.14	11.65	0.16	6.14	11.14	2.8	0.36	0.14	0.59	99.96
3-8ii	Mog	72.7	42.30	0.34	7.32	12.98	0.17	27.64	3.40	0.23	0.06	0.05	6.92	101.42
4-3	Mog	71.2	37.75	0.06	4.32	16.10	0.16	31.85	1.23	0.01	0.03	0.01	9.07	100.59
4-4	Mog	70.7	47.13	0.05	7.46	12.97	0.24	25.09	2.88	0.06	0.03	0	4.84	100.75
4-13	Mog	71.5	46.86	0.79	8.57	10.3	0.14	20.68	8.63	0.7	0.11	0.18	3.87	100.81
4-17	Mh	70.0	38.48	0.03	6.93	16.03	0.18	29.97	1.12	0.02	0.03	0.01	8.11	100.91
RLAe	Mh	72.7	39.07	0.10	2.35	15.02	0.16	32.01	1.97	0	0.02	0	10.39	101.09
RLAn	Mog	72.5	44.12	0.10	4.17	14.00	0.15	29.52	1.78	0.02	0.03	0.01	7.22	101.11

$Fe_2O_3^t$ – total iron as Fe_2O_3; LOI[1] – Loss on ignition; Mg# - magnesium number; Rock types: Mg- metagabbronorites; Mog – meta-olivine gabbronorite; Mh – metaharzburgite, Mt – metatroctolite; Bodies: DRT – Durhamtown; BC – Bethesda Church; F – Flatwoods; NQ – Norman Quarry; B.F.; – Bakers Ferry; NBF – North Bakers Ferry; N.H. – Nancy Hart complex.

Table 3. Bulk-rock trace element abundances in RLA rocks.

Sample	Type	Body	V	Cr	Ni	Cu	Zn	Rb	Sr	Y	Zr	Nb	Ba	Th	Ce	La	Pb
17-3N	Mg	DRT	247	430	106	80	50	36	262	13	40		169	3	97	15	4
17-3NN	Mg	DRT	258	394	129	7	95	13	209	11	32	2	67	nd	97	19	5
17-3SN	Mg	DRT	168	595	120	6	51	26	149	14	44	3	231	1	94	15	5
17-3SS1	Mog	DRT	261	854	148	40	54	17	287	13	45	3	87	nd	111	21	3
17-3SS2	Mog	DRT	267	785	141	39	56	15	244	11	37	2	177	nd	71	12	4
17-3SS3	Mg	DRT	221	214	92	43	48	19	443	11	35	2	174	1	96	15	5
RC20	Mg	DRT	186	266	100	13	41	16	230	12	31	4	119	nd	85	19	5
RC22	Mg	DRT	225	684	138	39	43	20	177	9	38	3	166	1	79	7	4
RC23	Mg	DRT	173	590	115	2	47	29	157	14	53	3	331	2	76	20	5
RC25	Mg	DRT	292	465	87	27	61	29	375	13	69	4	291	2	91	50	4

DRTCMG	Mg	DRT	218	252	72	29	66	11	187	21	53	3	155	nd	74	24	7
8-2A	Mh	F	28	383	506	1	84	8	7	3	8	1	nd	nd	84	nd	3
8-2B	Mog	F	35	622	368	6	70	9	146	2	6	1	nd	nd	88	nd	4
8-4A	Mg	F	247	84	43	54	38	8	638	13	67	4	15	nd	93	4	4
8-4B	Mog	F	27	483	316	7	81	19	216	3	6	1	188	1	80	nd	3
8-4C	Mog	F	9	137	325	4	86	14	270	1	6	1	88	nd	85	10	3
8-6A	Mog	F	30	40	424	55	121	9	46	2	8	1	Nd	nd	94	4	2
8-6Ci	Mog	F	42	189	461	46	101	9	177	2	7	nd	37	nd	89	5	3
8-7D	Mg	F	277	173	62	736	57	9	249	12	21	1	61	nd	70	5	5
BC1	Mg	BC	196	664	99	9	59	27	290	14	41	3	350	2	89	23	7
BC2	Mg	BC	280	1428	97	17	72	15	339	16	43	3	153	nd	111	20	5
BC3	Mg	BC	221	1397	126	26	56	23	280	11	46	2	267	1	79	15	5
BC4	Mg	BC	246	606	116	28	52	21	299	10	33	2	166	1	92	24	5
BC5	Mog	BC	236	1054	154	27	64	13	332	01	41	2	159	nd	98	17	6
BC6	Mog	BC	254	775	126	26	62	22	328	13	48	3	166	1	104	26	6
NQLPG	Mog	NQ	63	795	324	9	71	9	239	2	6	nd	nd	nd	91	nd	3
NQEPN	Mog	NQ	66	727	293	45	68	9	276	3	7	1	nd	nd	90	nd	4
NQNE	Mog	NQ	62	762	355	39	77	9	184	3	7	nd	nd	nd	89	6	3
3-10A	Mog	B.F.	0	30	217	4	72	8	177	1	5	nd	102	nd	53	1	2
3-10Bi	Mog	B.F.	nd	30	248	3	85	9	167	1	6	1	95	nd	49	nd	2
3-10Bii	Mt	B.F.	7	32	241	3	79	10	169	2	9	1	109	nd	50	nd	6
3-10D	Mt	B.F.	204	252	131	57	88	13	264	1	7	1	159	nd	49	5	3
3-10E	Mog	B.F.	4	36	243	6	77	9	156	1	6	nd	110	nd	52	nd	4
3-10F	Mt	B.F.	6	11	222	1	116	8	280	1	7	1	102	nd	50	nd	2
3-10G	Mog	B.F.	1	23	262	13	89	9	33	1	7	nd	95	nd	56	nd	3
3-10MW	Mog	B.F.	1017	66	76	339	41	14	510	6	11	1	138	nd	41	nd	5
3-10NEC	Mt	B.F.	3	15	98	3	45	10	635	1	6	1	103	nd	50	nd	5
3-10W	Mog	B.F.	0	24	309	1	77	8	10	1	7	1	98	nd	53	nd	3
Bell1	Mog	N.H.	30	672	564	124	83	8	3	1	7	1	93	nd	57	6	2
Bell2	Mog	N.H.	15	491	606	10	102	8	4	2	7	1	101	nd	55	nd	2
Bell3	Mog	N.H.	18	436	564	14	102	9	4	1	7	nd	107	nd	48	nd	4
Bell4	Mh	N.H.	19	552	568	17	96	8	2	1	6	1	nd	nd	92	nd	2
BellN1	Mog	N.H.	35	792	442	157	77	10	109	2	6	nd	nd	nd	93	nd	4
BellN2	Mog	N.H.	67	1014	616	1356	55	8	12	3	9	1	94	nd	48	nd	3
BellN3	Mog	N.H.	219	216	25	4	75	9	310	25	31	nd	89	nd	65	3	2
RRN	Mh	N.H.	9	141	513	64	100	9	95	1	7	nd	nd	nd	93	2	3
3-6	Mog	-	138	2035	1114	56	154	9	47	16	67	2	189	nd	64	21	1
3-8i	Mog	NBF	404	51	23	92	64	12	500	18	41	2	163	nd	43	3	4
3-8ii	Mog	NBF	65	1499	768	29	141	8	69	7	27	1	88	nd	55	2	2
4-3	Mog	-	40	1692	803	51	135	8	7	2	7	1	97	nd	57	3	5
4-4	Mog	-	22	1821	733	6	133	8	9	3	8	1	82	nd	60	1	2
4-13	Mog	-	162	1405	677	41	106	8	75	15	53	3	98	nd	98	30	3
4-17	Mh	-	7	38	575	1	117	8	11	2	7	1	110	nd	51	nd	2
RLAe	Mh	R.L.	65	2582	850	11	112	8	17	2	8	1	99	nd	52	nd	2
RLAn	Mog	R.L.	52	2282	699	39	96	8	4	2	8	1	104	nd	49	nd	3

nd – not detected, Mg- metagabbronorites; Mog – meta-olivine gabbronorite; Mh – metaharzburgite; Mt – metatroctolite; Bodies: DRT – Durhamtown; BC – Bethesda Church, F – Flatwoods; NQ – Norman Quarry; B.F. – Bakers Ferry, NBF – North Bakers Ferry; N.H. – Nancy Hart; R.L. – Russell Lake.

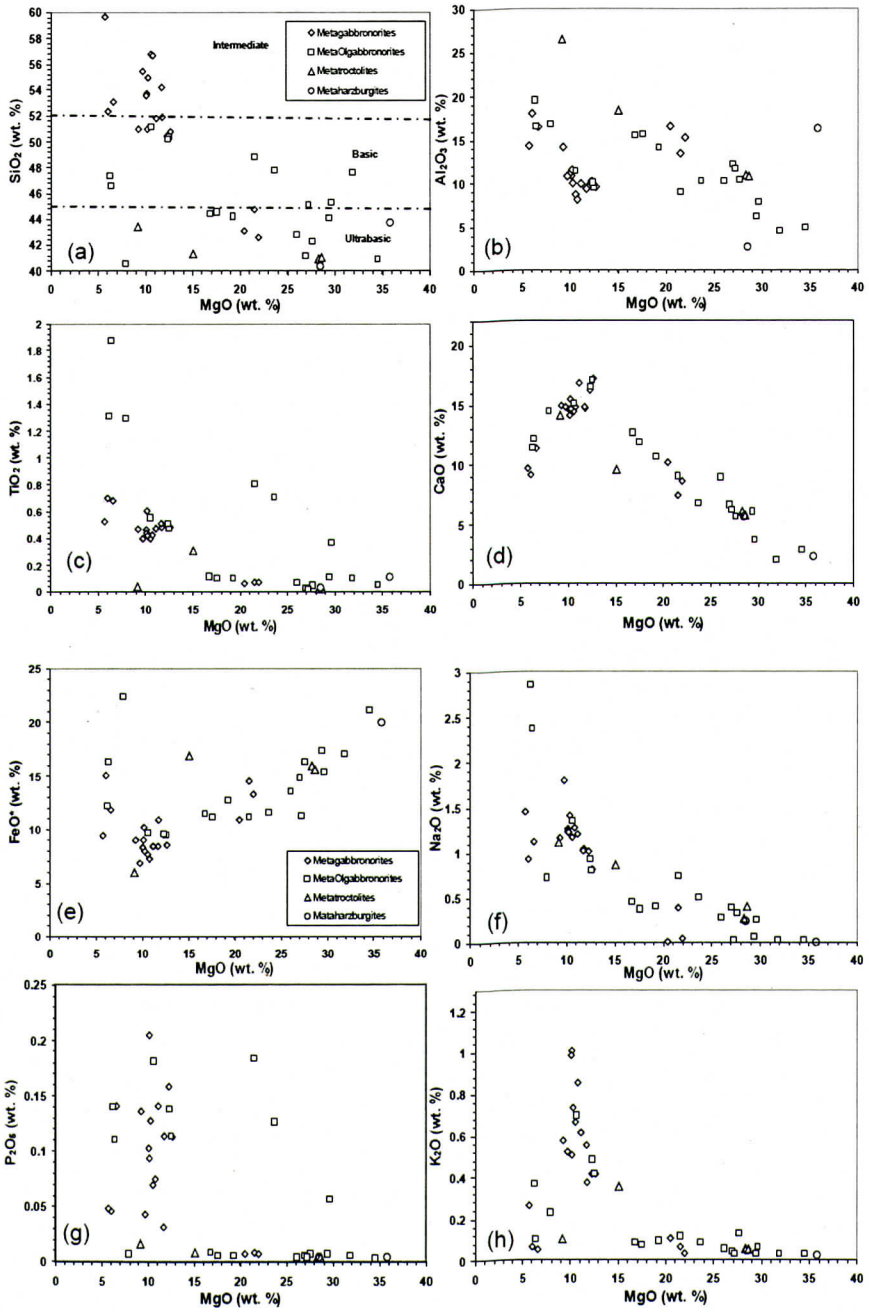

Figure 10. Plot of wt. % SiO_2 (a), wt.% Al_2O_3 (b), wt. TiO_2 (c), wt.% CaO (d), total iron as wt.% FeO* (e), wt.% Na_2O (f), wt.% P_2O_5 (g), and wt. % K_2O (h) *versus* wt.% MgO for samples from the study area. MDL = 0.01 wt.% for all oxides.

metagabbronorites and olivine metagabbronorites, with the bulk of the analyses falling between 7 and 20 wt.%. In metaharzburgite samples, Al_2O_3 contents are lower than in metagabbros, typically with concentrations below 7 wt.% (Fig. 10b). Metagabbroic rock samples with TiO_2 contents higher than approximately 1.3 wt.% have less than approximately 10 wt.% MgO (Fig. 10c). Most of the metaharzburgites and metatroctolites samples from the RLA with magnesia contents higher than 30 wt.% have TiO_2 contents at or below detection limits (Fig. 10c).

Calcium oxide concentrations ranges from values of approximately 2 wt.% in olivine metagabbronorite and metaharzburgite samples with MgO contents of over 30 wt.% to values as high as 17 wt.% in metagabbroic samples with MgO values of approximately 12 wt.% (Fig. 10d). A negative correlation between MgO and CaO is observed when MgO is greater than approximately 12 wt.%, but samples with lower MgO values than approximately 12 wt.% define a positive correlation between CaO and MgO (Fig. 10d).

Total iron varies between approximately 4 wt.% in metagabbronorites and 25 wt.% in olivine metagabbronorites, metatroctolites, and metaharzburgites (Fig. 10e). For most samples FeO* and MgO are positively correlated but a few olivine metagabbronorite samples with relatively low MgO have high FeO contents and plot off the correlation (Fig. 10e). In rocks from the study area, no correlation is observed between the oxides MnO and MgO (not shown), and only a poor positive correlation between FeO* and MnO exists.

Sodium is a major constituent of feldspars and its concentration in protoliths of the RLA is probably controlled by the occurrence and proportion of feldspars. In the investigated area, Na_2O ranges from values below detection limits in metaharzburgite and olivine metagabbronorite samples with MgO values greater than 24 wt.%, to values close to 4 wt.% in metagabbroic samples with MgO values less than 7 wt.% (Fig. 10f).

Phosphorous, K and Ti are incompatible elements in mafic magmas, and their behavior in the RLA rocks is consistent with that generalization. Phosphorous varies from values below detection limits in metaharzburgite and olivine metagabbronorite samples with MgO values of over 30 wt.%, to values of approximately 0.2 wt.% in metagabbroic samples with MgO values of 10 wt.% (Fig. 10g). The range in P_2O_5 concentrations in RLA samples is limited, from 0.1 – 0.2 wt.%. Likewise, K_2O varies from values at or below detection limits in metaharzburgite and olivine metagabbronorite samples with MgO values greater than 16 wt.%, to values as high as 1.18 wt.% in a metagabbronorite with an MgO value of 9.81 wt.% (Fig. 10h).

TRACE ELEMENT ABUNDANCES

Bulk-rock trace element abundances from the RLA are shown in Table 3. The variation of the element chromium is plotted *versus* the oxide MgO in Fig. 11a. The highest Cr concentration in the RLA (2582 ppm) occurs in a sample with the highest MgO (35.82 wt.%) content - a metaharzburgite from the RLA type area. There is a poor positive correlation between Cr and MgO as shown in Fig. 11a. Samples from Bakers Ferry body, where the only spinel-bearing body from the study area has been observed, have Cr concentrations of less than 70 ppm, with one "outlier" having a relatively higher value of 252 ppm. However, the spinels in these rocks are Cr-poor (Chaumba, 2009).

Nickel is concentrated in Fe-Mg silicates, especially olivine and sulfides (e.g., Frey and others, 1978; Cox and others, 1979; Hart and Dunn, 1993). Thus, if igneous bulk compositions were preserved, then Ni should vary in a positive way with MgO (Fig. 11b). For MgO values less than 21 wt.% MgO, a strong positive correlation is observed for the RLA samples (Fig. 11b), but at higher MgO values, this relationship breaks down and no correlation is observed due to the inferred cumulate nature of rocks with high MgO contents as discussed below. A plot of Cr versus Ni (not shown), which is useful in identifying the Fe-Mg silicates present, reveals that 44 of the 55 RLA samples plot closer to the Cr rather than to the Ni axis. Almost all metagabbroic rocks plot closer to the

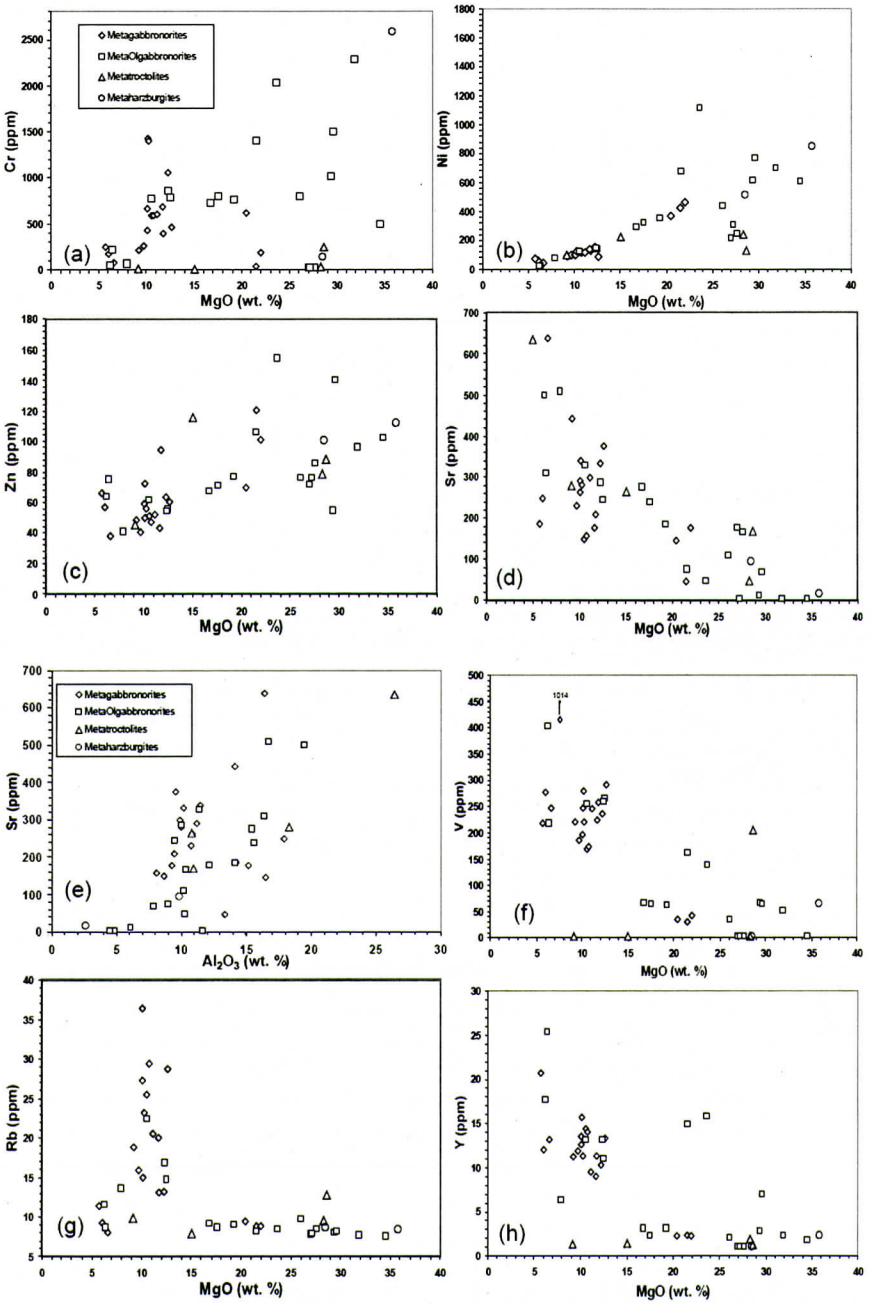

Figure 11. Plot of ppm Cr (a), ppm Ni (b), ppm Zn (c), and ppm Sr (d) *versus* wt.% MgO for samples from the study area. Plot of ppm Sr *versus* wt.% Al_2O_3 (e) showing a weak positive correlation between the two. Plot of ppm V (f), ppm Rb (g), and ppm Y (h) *versus* wt.% MgO for samples from the study area.

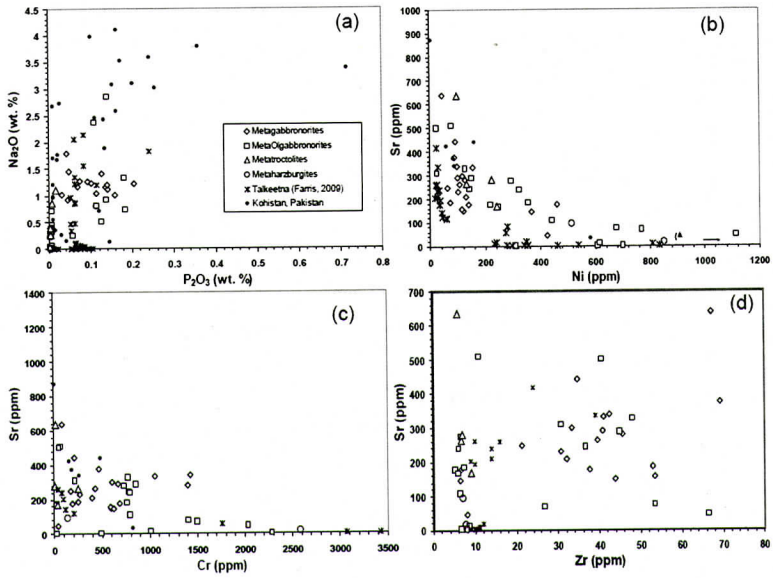

Figure 12. Plot of Na_2O (wt. %) versus P_2O_5 (wt.%) (a), Sr versus Ni (b), Sr versus Cr (c), and Sr versus Zr (d). Kohistan data from Khan et al (1989) and Miller and Christensen (1994).

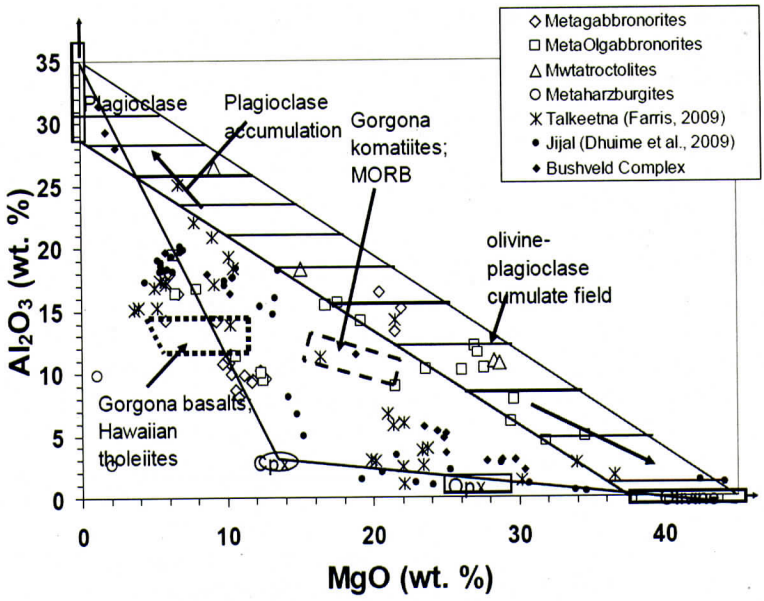

Figure 13. Plot of wt.% Al_2O_3 *versus* wt.% MgO for samples from the study area. The cumulate triangle apices (e.g., Peterson & Ryan, 2009) are defined by olivine, plagioclase, and cpx (clinopyroxene) compositions after Bryan (1979), Frey and Clague (1983), Schilling and others (1983), Thornber (2001), and Godard and others (2009). Fields for high-Mg melts such komatiites and typical upper mantle magmas such as Hawaiian tholeiites (e.g., Thornber, 2001) and basaltic komatiites are also shown. Mid-ocean ridge basalts (e.g., Schilling and others, 1983; Frey and others, 1974; Niu & O'Hara, 2008) also plot in the Gorgona basalts field (Echeverria, 1980). Fields of Gorgona rocks from Echeverria (1980). Metatroctolites plot in the plagioclase-olivine cumulate field shown. Kohistan data from Khan et al (1989) and Miller and Christensen (1994). Bushveld Complex data from Maier and others (2000).

Cr axis whereas almost all metatroctolites plot closer to the Ni axis. Zn also can be concentrated in olivine (Paster and others, 1978) and Zn shows a positive correlation with MgO in RLA samples (Fig. 11c), consistent with olivine control. The highest Zn contents are over 120 ppm in metagabbroic rocks, with the lowest Zn concentrations being found in metagabbronorites and meta-olivine gabbronorites, samples with no or very low normative olivine.

Strontium contents can reflect the modal proportion of plagioclase in cumulate rocks (Cox and others, 1979; Irving, 1978, Frey and others, 1978). In metaharzburgite and olivine metagabbronorite samples with MgO contents greater than 30 wt.% MgO, Sr concentrations are at, or below, the detection limit, whereas in samples with MgO contents less than 30 wt.% MgO, a systematic increase in Sr with decreasing MgO contents occurs (Fig. 11d). The highest Sr concentration of approximately 640 ppm in RLA samples investigated occurs in a metagabbronorite sample (Fig. 11d). A weak positive correlation occurs between Sr and Al_2O_3 (Fig. 11e).

Three other elements, V, Rb, and Y, show concentration variations relative to MgO broadly consistent with incompatible elements (Figs. 11e, f, g; respectively). Vanadium shows a negative correlation with MgO: V varies from below detection limits to a high of over 1000 ppm in a metagabbronorite with an MgO content of 7.9 wt.% (Fig. 11e). Rubidium can be mobile during metamorphism (e.g., Pavlides, 1981; Rollinson, 1993). In the RLA, almost all samples with MgO values of greater than 15 wt.% MgO have Rb concentrations at or below detection limits as shown in Fig. 11f. Samples from the RLA with less than 15 wt.% MgO have highly variable Rb contents (~8 to ~35 ppm), with the highest Rb concentration of 36 ppm occurring in a metagabbronorite with 10 wt.% MgO (Fig. 11f).

Yttrium is a proxy for the heavy rare earth elements and relatively immobile during metamorphism/alteration (e.g., Rollinson, 1993). In the RLA, this element displays an abundance pattern similar to that of Rb (Fig. 11g) and has concentrations ranging from below the detection limit in most samples with MgO contents more than 30 wt.% MgO to concentrations as high as 25 ppm for samples with 5-15 wt.% MgO (Fig. 11g).

DISCUSSION

Results of field mapping and trenching carried out during this investigation are consistent with previous studies (McFarland, 1992; Allard and Whitney, 1994) that suggested that metamorphosed RLA rocks rest on underlying country rocks along a shallow subhorizontal contact. Shearing, observed in some cases in rocks of the RLA as well as underlying country rocks near the contacts between the two units (e.g., Russell Lake type locality), lend support to the idea that rocks of the RLA were tectonically emplaced onto the country rocks (Allard and Whitney, 1994) and supports (e.g., Kusky and others, 2011) an ophiolite origin for these rocks. Tectonic emplacement is also consistent with the lack of chilled margins within the RLA bodies. The lack of strong shearing at the base of some bodies remains a problem for the thrust hypothesis. However, it is also possible that some bodies (such as Durhamtown) which lack basal shearing are located at the margins of the RLA thrust sheet where the sheet came to rest on underlying rocks. Further, it must be noted that contacts between the RLA and their country rocks are not always exposed.

Some RLA rocks preserve relict igneous textures including cumulate textures at hand sample scale, and relict igneous layering which suggests that at least some of the rocks formed as igneous cumulates and were later metamorphosed possibly during orogenic events that affected the Appalachian mountain belt. The occurrence of both relict cumulate textures and layering in rocks under investigation lends support (e.g., Dilek and Furnes, 2011; Kusky and others, 2011) to an ophiolite origin for the RLA. A key question regarding the interpretation of these rocks is whether or not the present bulk compositions can be used to infer petrogenesis. The normative calculations show that the bulk compositions of the majority of the samples are comparable to gabbroic rocks of various sorts

(Fig. 5), and the range to very high MgO contents in some rocks (as well as the cumulate textures) are consistent with the accumulation of Fe-Mg silicates in a magma chamber. Moreover the correlation of Ni with MgO (Fig. 11) is consistent with olivine control, and the very high Cr contents of some rocks are consistent with spinel accumulation. Approximately half the samples we analyzed have MgO contents in excess of 15 wt.%, consistent with an origin as metacumulates; however there are many samples with MgO contents near 10 wt% indicating an origin as crystallized basaltic magma (Fig. 13). Although it is clear based on high LOI that many of the rocks were open to at least H_2O during metamorphism, we argue based on oxide and element abundance patterns such as those of MgO, Ni and Cr (Figs. 10 and 11), that the bulk compositions reflect igneous processes and can be used to infer petrogenesis.

An assessment of the suitability of the data for igneous interpretation can be made by plotting the variation of elements that are mobile during metamorphism from the present study and compare the trends to those from rocks that have undergone very little metamorphism or alteration from possible comparable tectonic settings, such as the Talkeetna arc in Alaska (e.g., Farris, 2009) and the Kohistan arc (e.g., Khan and others, 1989; Miller and Christensen, 1994) (Fig. 12). It can be seen in Fig. 12a that generally incompatible oxides such as potassium and sodium are poorly correlated, but are comparable to those from Talkeetna and Kohistan. A plot of a moderately incompatible element such as Sr versus a compatible element such as Ni shows a negative trend broadly comparable to other island arc complexes (Fig. 12b). Cr behaves in a similar manner to Ni and shows a broadly comparable trend when plotted versus Sr (Fig. 12c). A plot of two generally incompatible elements like Sr and Zr shows no correlation, not very different from the trend displayed by Talkeetna data (Fig. 12d), although modal plagioclase strongly influences the trend on such a plot. Thus, as shown in Fig. 12, trends displayed by data from the present study are comparable to those from island arc settings.

Consequently, many of the RLA rocks appear to be metacumulate rocks, and are broadly comparable to rocks from island arc complexes such as the Kohistan complex in northern Pakistan (e.g., Khan and others, 1989; Miller and Christensen, 1994; Petterson, 2010) and Talkeetna and Kodiak Talkeetna arc in Alaska (e.g., Farris, 2009). In cumulate rocks, the cumulate minerals plus interstitial melt control the bulk-rock compositions. In the RLA rocks, metamorphism has complicated this simple relationship but bulk compositions are preserved well enough to infer a cumulate protolith for many RLA rocks. For example, in a plot of Al_2O_3 versus MgO many of the RLA rocks plot within the plagioclase-olivine field (Fig. 13) consistent with an adcumulate origin; others plot near this field but displaced towards lower MgO consistent with the incorporation of some interstitial melt. Other samples plot along the clinopyroxene-plagioclase join and near the field for modern MORB and Hawaiian tholeiites suggesting that these rocks represent frozen gabbros. For some of these rocks their bulk compositions are displaced towards plagioclase or clinopyroxene indicating that the gabbros may have included accumulated plagioclase or clinopyroxene.

Further evidence of the original cumulate nature of rocks of the RLA is presented in Figs. 14 and 15. A highly compatible trace element (e.g., Ni) is plotted *versus* magnesium oxide in Fig. 14. The occurrence of high Ni contents coupled with much higher MgO contents than those typically found in magmas such as MORB and tholeiites is consistent with the concentration of Ni in cumulate olivine (e.g., Rollinson, 1993). Similarly, elevated Sr combined with high Al_2O_3 in a few RLA rocks compared to melts such as MORB and tholeiites shown in Fig. 15 point towards cumulate plagioclase in these rocks because Sr substitutes for Ca in plagioclase; thus cumulate plagioclase could cause the high concentrations of Sr in RLA rocks (Fig. 15). Rocks from the Kohistan and Kodiak Talkeetna arcs have similar Sr and Al_2O_3 contents.

Chromium contents also hint at a cumulate origin for some rocks of the RLA. Many of the rocks have more than 1000 ppm Cr (Fig. 11), and that observation in conjunction with high

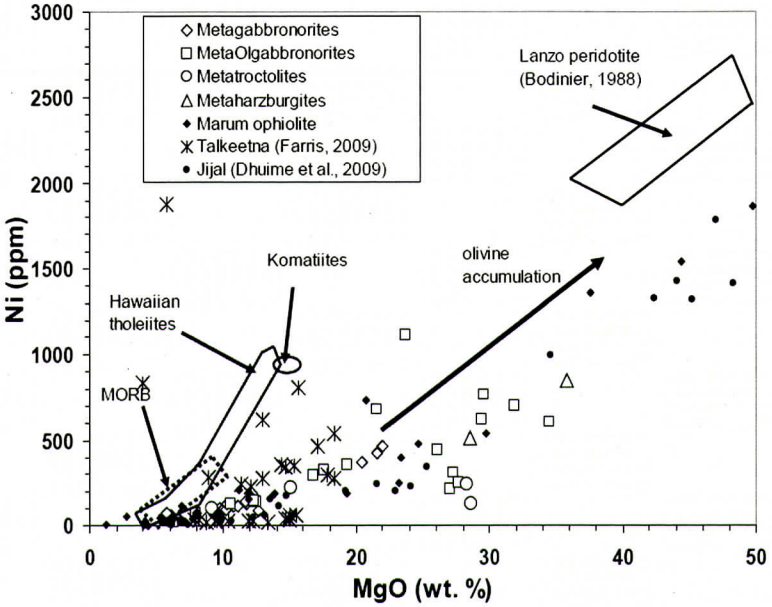

Figure 14. Plot of ppm Ni *versus* wt.% MgO for samples from the study area. Fields for high-Mg melts such komatiites and typical upper mantle melts such as tholeiites and basaltic komatiites are also shown. Field for normal mid-ocean ridge basalts (e.g., Thornber, 2001), Hawaiian tholeiites (Niu & O'Hara, 2008; West and others, 1992) and Gorgona komatiites (Gansser and others, 1979) are also shown. Marum ophiolite (Jaques and others, 1983) and Lanzo (Bodinier, 1988) data are shown for comparative purposes. Kohistan data from Khan and others (1989).

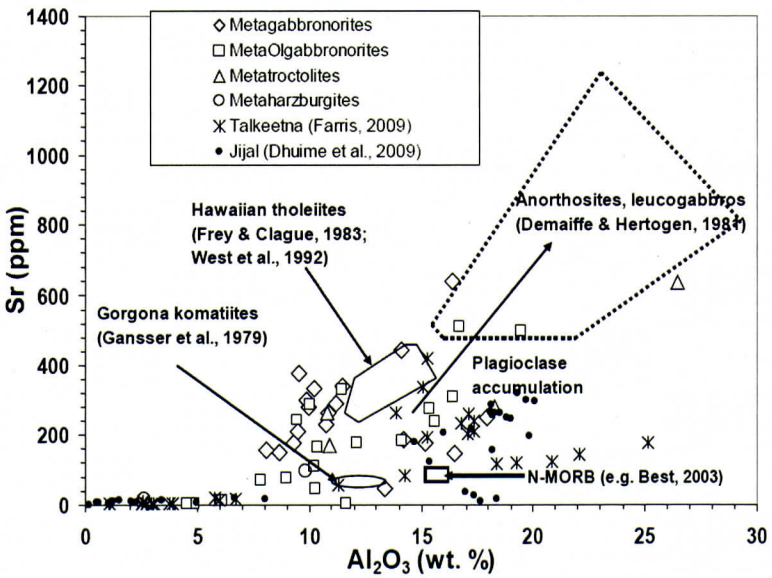

Figure 15. Plot of ppm Sr *versus* wt.% Al_2O_3 for samples from the study area. Fields for high-Mg melts such komatiites and typical upper mantle melts such as tholeiites and basaltic komatiites are also shown. Field for normal MORB (e.g., Best, 2003), Hawaiian tholeiites (Frey and Clague, 1983; West and others, 1992) and Gorgona komatiites (Gansser and others, 1979) are shown for comparison purposes. Kohistan data from Khan et al (1989).

MgO (>20 wt.%) for many of these (but not all) rocks are consistent with cumulate chromite accompanying cumulate olivine in the original rocks. Very few chromite grains were observed under the microscope, and a few chromite grains were observed under the microprobe. FeO and Zn concentrations in the chromites are high (~21.21 and 0.14%, respectively, Chaumba, 2009), and Ni contents are low (< 0.1%, Chaumba, 2009), chemical signatures that are consistent with chromites metamorphosed under amphibolite facies conditions (Barnes, 2000). It is possible that some of the chromite grains in RLA samples were replaced by magnetite, probably due to incomplete metamorphic reaction between chromite and chlorite-bearing silicate assemblages during amphibolite facies metamorphism (e.g., Barnes, 2000).

Thus the variation in three key trace elements (Sr, Cr, and Ni) in conjunction with MgO and Al_2O_3 (Fig. 13) support the idea that some of the rocks were originally cumulate rocks rich in plagioclase, olivine, and chromite and perhaps clinopyroxene that underwent nearly isochemical metamorphism (with the exception of H_2O). Rare relic cumulate textures support this contention. Additionally, many of the rocks have bulk compositions similar to basaltic magmas (Fig. 13), and thus the rocks of the RLA are not simply cumulates but include rocks which were originally intrusive gabbros – the lack of chill margins and contact metamorphism as described above shows that they were not intrusive into their current country rocks. The observation that the majority of RLA samples plot closer to the Cr rather the Ni axis indicates that these rocks are dominated by pyroxenes and amphiboles relative to olivine, further lending support to an island arc origin.

Tectonic discrimination diagrams utilizing 'immobile' trace elements point to formation of RLA rocks in a subduction zone setting - the volcanic arc field shown in Fig. 16. Only metagabbroic rocks were plotted in Fig. 16, since cumulate rocks are rocks formed from crystal accumulation and are not good indicators of tectonic settings (e.g., Pearce, 1983). Suprasubduction-zone basaltic magma compositions are characterized by elevated concentrations of large ion lithophile elements (LILE: Cs, Rb, Ba, Th, K, Sr, Pb) relative to high field strength elements (HFSE: Nb, Ta, Hf, Zr, Ti) (e.g. Pearce and others, 1984). Models of subduction-zone hold that fluids and/or siliceous melts derived from the subducting oceanic slab carry high concentrations of LILE (±light rare earth elements {LREEs}) that metasomatize the overlying mantle wedge and aid in lowering liquidus temperatures. Subduction fluids may carry elemental contributions from a variety of subducted sediments in addition to contributions from the slab itself (i.e., dehydration reactions in altered oceanic crust). HFSE and heavy rare earth elements (HREE) concentrations tend to be controlled primarily by the composition of the mantle wedge prior to metasomatism. This results in the trace-element signatures of subduction-related magmas that appear to be derived from three main sources: 1. the subducted oceanic lithosphere, 2. subducted sediment, and 3. the mantle wedge overlying the subducting slab (e.g., Davidson, 1996). Superimposed on conservative mantle wedge-derived components (Nb, Zr, Sm, Eu, Ti, Dy, Y, Yb, Lu) are elevated concentrations of slab-derived components (Cs, Rb, Ba, Th, U, K, La, Ce, Pb, Sr) that produces the distinctive pattern of "troughs" and "spikes" that is characteristic of suprasubduction-zone magmas as shown in Fig. 17 (e.g., Metcalf and Shervais, 2008; Schuth and others, 2009). Spidergrams for RLA samples show negative Nb depletions (Fig. 17), which is consistent with formation of these rocks in a subduction zone setting. Trends shown by the data in Fig. 17 can be produced by contamination of island arc magmas by either upper crust or lower crust, or both.

The P-T conditions for the cores of the hornblendes rocks under investigation are consistent with the development of corona textures in these rocks since the reaction occurs at pressures of at least 8 kbars (e.g., Kushiro and Yoder, 1966; Tomilenko and Kovyazin, 2008). Such pressures are consistent with an island arc rather than a MORB origin for the RLA. It has been reported that subarc lithosphere is dominated by a residual refractory mantle of harzburgite composition, not lherzolite (e.g., Metcalf and Sher-

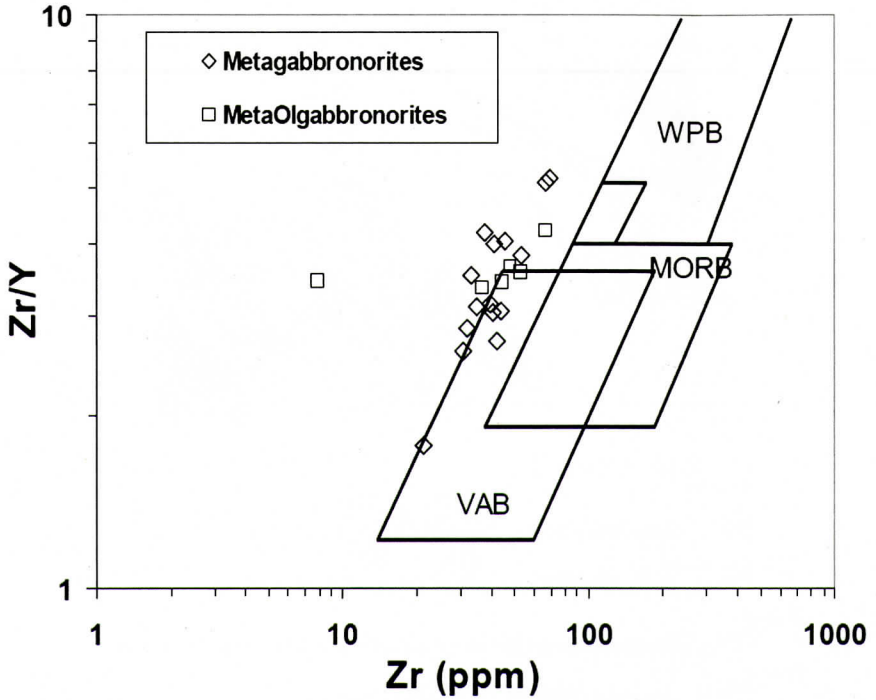

Figure 16. Tectonic discrimination diagram for RLA metagabbroic rocks based upon Zr/Y versus Zr (ppm). Abbreviations: WPB – within plate basalts, MORB – mid-ocean ridge basalt, and VAB – volcanic arc basalts (after Pearce, 1983). Some RLA samples plot only within the VAB field, whereas the rest plot outside any field.

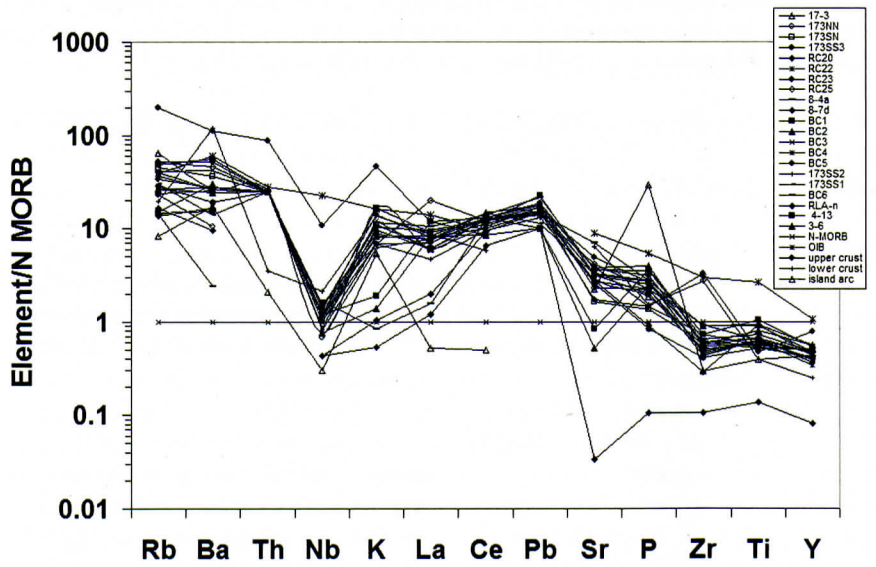

Figure 17. Spidergram for trace element concentrations for RLA samples normalized to normal mid-ocean ridge basalt (N-MORB) and arranged in order of increasing incompatibility with respect to mantle mineralogy (e.g., Rollinson, 1993). Normalization values are from Sun and McDonough (1989). Note that RLA samples show negative Nb anomalies, suggesting formation in a subduction zone environment.

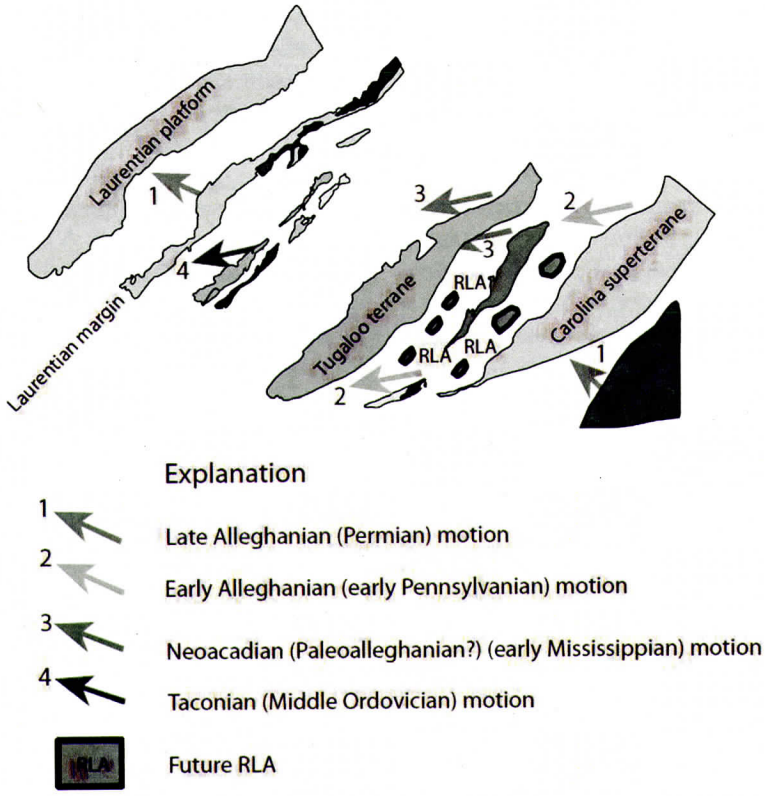

Figure 18. Retrodeformed tectonostratigraphic terranes in the southern Appalachians with numerous island arcs scattered in the proto-Atlantic ocean between Gondwana extending to west of the Tugaloo terrane which gave rise to the RLA (modified from Hatcher and others, 2007). Arrows indicated are numbered to show accretion timing.

vais, 2008). In contrast, suboceanic lithosphere is dominated by lherzolite, which is thought to represent smaller degrees of partial melting of a MORB asthenosphere source (e.g., Dick, 1989). Very few ultramafic rocks occur in the RLA - metagabbroic rocks, are volumetrically dominant (Fig. 4). The absence of lherzolites, and the relative volumes of metaharzburgites, metatroctolites, and metagabbroic rocks in the RLA suggests that the RLA may be composed primarily of compositionally diverse cumulate rocks (here dominated by gabbroic rocks) consistent with formation in island arc settings (e.g., Metcalf and Shervais, 2008). Further, the position of the RLA in an orogenic belt may also lend support to an island arc origin for these rocks. Shervais (2001), for example, concluded that a normal part of the evolution of these ophiolitic rock assemblages (such as the RLA) involved emplacement onto the leading edge of partially subducted continental margins (Tethyan ophiolites) or exposure by accretionary uplift along an active plate margin (Cordilleran ophiolites).

Hatcher and others (2007) recently summarized the development of the southern Appalachians as chiefly resulting from the movements of the continents of North America and Africa during the final stages of the formation of Pangea. Of particular importance were the accumulation of accreted terranes between the two continents which gave rise to the Carolina superterrane, Cat Square terrane, Tugaloo terrane and others (Fig. 18). As the proto-Atlantic ocean closed during the Alleghanian orogeny (e.g., Hatcher and others, 2007), we suggest that some island arc fragments scattered in that ocean started colliding with each other (Fig. 19)

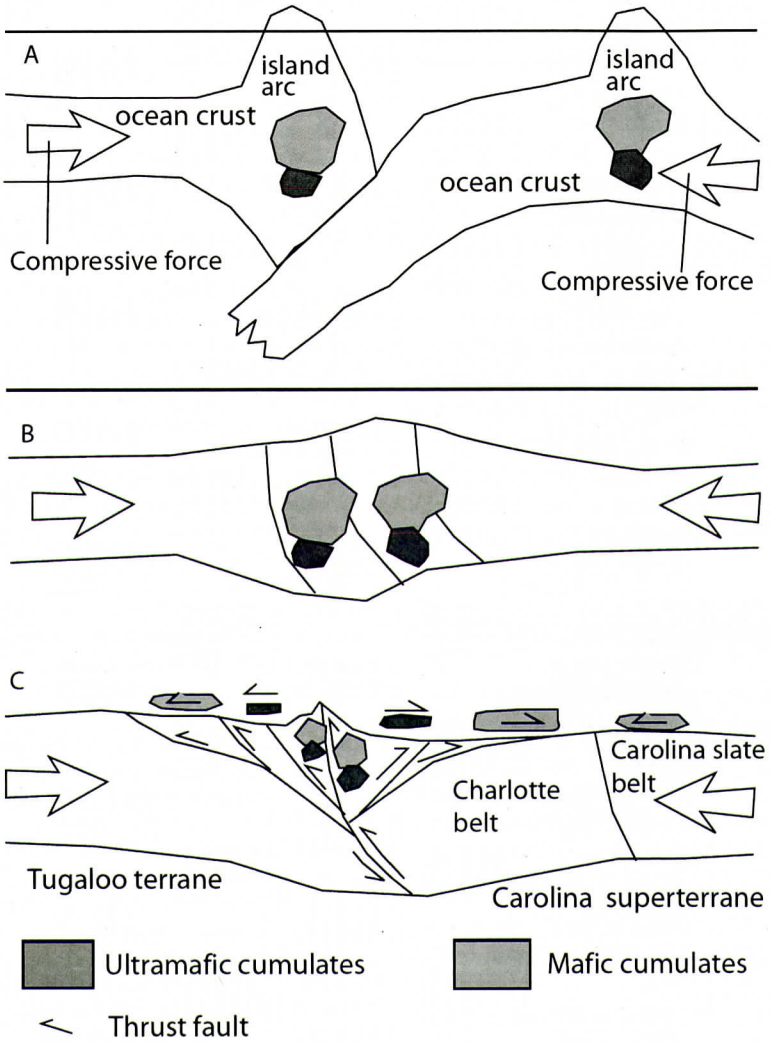

Figure 19. Cartoon illustrating the envisaged events that led to development of the RLA. A. Arc-arc collision during initial stages of the assembly of Pangea, B. Development of corona textures due to high-pressure metamorphism resulting from arc-arc collision, C. Thrusting of the RLA onto its present position due to collision of various arcs during final assembly of Pangea.

as the ocean floor on which they were constructed was consumed at subduction zones. The arc-arc collisions led to high-pressure metamorphism due to burial during arc-arc collision as shown in Fig. 19. Some of the island arcs were probably located between the Tugaloo terrane and Carolina superterrane, whereas other island arcs were probably located between the Carolina superterrane and Gondwanaland as shown in Fig. 18.

CONCLUSIONS

The rocks of the RLA retain igneous compositions in most cases, and the preserved bulk compositions are consistent with a suite of rocks dominated by gabbroic to metatroctolitic cumulates, with lesser amounts of gabbroic in-

trusives and relatively minor ultramafic cumulates. All the RLA rocks have a similar petrogenesis consistent with the idea of Allard and Whitney (1994) that the rocks constitute klippe from a widespread thrust sheet in the Carolina superterrane. The lack of evolved compositions and the high MgO and CaO contents of many of the metacumulates suggest that these rocks originated within oceanic lithosphere with the most likely environment being an oceanic island arc. As such these rocks constitute fragments of a dismembered ophiolite although the key point is their origin within an ocean basin. Following Hatcher and others (2007), we infer that these rocks were emplaced during the Alleghanian orogeny as an island arc(s) was compressed and thrust over continental crust when Africa and North America collided.

ACKNOWLDGEMENTS

Some of the expenses for field work and analytical costs of this work were supported by a Geological Society of America student research grant, the Watts-Wheeler Fund, and the Allard Award at the University of Georgia, which are gratefully acknowledged. We thank Drew Coleman, Doug Crowe, Alberto Patino-Douce, and Sam Swanson for reviewing this work at various stages. Very helpful comments from David Farris and Brent Owens substantially improved the manuscript. Sam Swanson alerted us to the importance of considering normative corundum as an indicator of metasomatism. Steve Clark, Mariela Noguera, Heath McGregor, Dan Bulger, Sheldon Skaggs and Jay Austin helped with fieldwork. Doug Dvoracek helped with XRF analyses.

REFERENCES

Allard, G.O. and Whitney, J.A., 1994, *Geology of the Inner Piedmont, Carolina Terrane, and Modoc Zone in Northeastern Georgia*, Georgia Geological Survey, Project Report 20, 36 p.

Allard, G. and Whitney, J., 1995, The Russell Lake Allochthon – a neglected tectonostratigraphic unit in the southern Appalachians, *South Carolina Geology*, v. 38, p. 71-77.

Barnes, S.J., 2000, Chromite in komatiites, II. modification during greenschist to mid-amphibolite facies metamorphism, *Journal of Petrology*, v. 41, p. 387-409.

Berger, S., Cochrane, D., Simons, K, Savov, I., Ryan, J.G. & Peterson, V.L., 2001, Insights from rare earths elements into the genesis of the Buck Creek complex, Clay County, NC, *Southeastern Geology*, v. 40, p. 201-212.

Best, M.G., 2003, *Igneous and Metamorphic Petrology*, Blackwell, Maden, Massachusetts, 729 p.

Bodinier, J.L., 1988, Geochemistry and petrogenesis of the Lanzo peridotite body, western Alps, *Tectonophysics*, v. 149, p. 67-88.

Bryan, W.B., 1979, Regional variation and petrogenesis of basalt glasses from the FAMOUS area, Mid-Atlantic Ridge, *Journal of Petrology*, v. 20, p. 293-325.

Carpenter, J.R. & Phyfer, D.W., 1969, Proposed origin for the alpine type ultramafics of the Appalachians, *Geological Society of America, Abstracts with Programs*, v. 1, p. 261-263.

Chaumba, J.B., 2009, *The Russell Lake Allochthon, Southern Appalachians: structure, petrography, bulk-rock and mineral chemistry, O, H, and Sm-Nd isotope geochemistry*, Ph.D. Dissertation, University of Georgia, Athens, 390 p.

Chaumba, J.B., & Swanson, S.E., 2008, An evaluation of the use of bulk-rock geochemistry in determining igneous protoliths of rocks from the soapstone ridge complex, Atlanta, Georgia, *Geological society of America, Program with Abstracts*, v. 40, no. 4, p. 69.

Clippard, J.E. & Hawman, R.B., 1995, Shallow seismic reflection profiling over an ultramafic complex in the Carolina terrane, NE Georgia, *South Carolina Geology*, v. 38, p. 70-94.

Coleman, R.G., 1977, *Ophiolites: ancient oceanic lithosphere*, Springer-Verlag, New York, 229 p.

Cox, K.G., Bell. J.D. & Pankhurst, R.J., 1979, *The interpretation of igneous rocks*, George Allen & Unwin, London, 450 p.

Davidson, J.P., 1996, Deciphering mantle and crustal signatures in subduction zones magmatism, in: Bebout, G.E., School, D.W., Kirby, S.H., and Platt, J.P., eds., *Subduction Top to Bottom*: American Geophysical Union Geophysical Monograph 96, p. 251–262.

Demaiffe, D. & Hertogen, L., 1981, Rare earth element geochemistry and strontium isotopic composition of a massif-type anorthositic-charnockitic body; the Hidra Massif (Rogaland, SW Norway), *Geochimica et Cosmochimica Acta*, v. 45, no. 9, pp.1545-1561.

Dhuime, B., Bosch, D., Garrido, C. J., Bodinier, J.-L., Bruguier, O., Hussain, S. and Dawood, H., 2009, Geochemical architecture of the lower- to middle-crustal section of a paleoisland Arc (Kohistan complex, Jijal-Kamila area, N Pakistan): implications for the evolution of an oceanic subduction zone, *Journal of Petrology*, v. 50, p. 531-569.

Dilek, Y. and Furnes, H., 2011, Ophiolite genesis and global tectonics: Geochemical and tectonic fingerprinting of ancient oceanic lithosphere, *Geological Society of America Bulletin*, v. 123, p. 387-411.

Echeverria, L.M., 1980, Tertiary or Mesozoic komatiites from Gorgona island, Columbia: field relations and geochemistry, *Contributions to Mineralogy and Petrology*, v.73, p. 253-266.

Farris, D.W., 2009, Construction and evolution of the Kodiak Talkeetna island arc crustal section, *Crustal cross-sections from the western North America Cordillera and elsewhere: Implications for tectonic and petrologic processes, in:* Miller, R. and Snoke, A. (eds.), Geological Society of America Special Paper 456, p. 69-96.

Frey, F.A., Bryan, W.B. & Thompson, G., 1974, Atlantic ocean floor: geochemistry and petrology of basalts from Legs 2 and 3 of the Deep-Sea Drilling Project, *Journal of Geophysical Research*, v. 79, p. 5507-5527.

Frey, F.A., Green, D.H. & Roy, S.D., 1978, Integrated models of basalt petrogenesis: a study of quartz tholeiites to olivine melilitites from southeastern Australia utilizing geochemical and experimental petrological data, *Journal of Petrology*, v. 19, p. 463-515.

Frey, F.A. & Clague, D.A., 1983, Geochemistry of diverse basalt types from Loihi Seamount, Hawaii: petrogenetic implications, *Earth and Planetary Science Letters*, v.66, p. 337-355.

Gansser, A., Dietrich, V.J. & Cameron, W.E., 1979, Palaeogene komatiites from Gorgona Island, *Nature*, v.278, p. 545-546.

Gaudette, H.E., 1981, Zircon isotopic age from the Union ultramafic complex, Maine, *Canadian Journal of Earth Sciences*, v. 18, p. 405-409.

Godard, M., Awaji, S., Hansen, H., Hellebrand, E., Brunelli, D., Johnson, K., Yamasaki, T., Maeda, J., Abratis, M., Christie, D., Mariet, C. & Risner, M., 2009, Geochemistry of a long in-situ section of intrusive slow-spread oceanic lithosphere: results from IODP Site U1309 (Atlantis Massif, 30oN Mid-Atlantic-Ridge), *Earth and Planetary Science Letters*, v.279, p. 110-122.

Hart, S.R. & Dunn, T., 1993, Experimental cpx/melt partitioning of 24 trace elements, *Contributions to Mineralogy & Petrology*, v. 113, p. 1-8.

Hatcher, R.D., Jr., 2005, Southern and central Appalachians, in Selley, R.C., Cocks, R. & Plimer, I. (eds), Encyclopedia of geology, London, Elsevier Limited, p. 72-81.

Hatcher, R.D., Bream, B.R. & Mershat, A.J., 2007, Tectonic map of the southern and central Appalachians: a tale of three orogens and a complete Wilson cycle, in: *4-D framework of continental crust, Geological Society of America*, Boulder, Colorado, Memoir 200, p. 595-632.

Hess, H.H., 1955, Serpentinites, orogeny and epeirogeny, *in* Poldervaart, A. (ed), *Crust of the Earth*, Geological Society of America Special Paper 62, p. 391-408.

Hibbard, J., van Staal, C., Rankin, D., and Williams, H., 2006. *Geology, lithotectonic map of the Appalachian Orogen (South), Canada-United States of America*, Geological Survey of Canada, Map 02096A, scale 1:1500000.

Hooper, R.J., & Hatcher, R.J., Jr., 1989, The origin of ultramafic rocks from the Berner mafic complex, central Georgia, In: S.K. Mittwede & E.F. Stoddard (eds.), *Ultramafic rocks of the Appalachian Piedmont*, Geological Society of America, Special Paper 231, p. 87-92.

Jaques, A.L., Chappell, B.W. & Taylor, S.R., 1983, Geochemistry of cumulus peridotites and gabbros from the Marum ophiolite complex, northern Papua New Guinea, *Contributions to Mineralogy and Petrology*, v. 82, p. 154-164.

Kite, L.E. & Stoddard, E.F., 1984, The Halifax County complex: oceanic lithosphere in the eastern North Carolina Piedmont, *Geological Society of America Bulletin*, v. 95, p. 422-432.

Khan, M.A., Jan, M.Q., Windley, B.F., Tarney, J., & Thirlwall, M.F., 1989, The Chilas mafic-ultramafic complex; the root of the Kohistan island arc in the Himalaya of Northern Pakistan, in: L.L. Malinconico, Jr. & R.J. Lillie (eds.), *Tectonics of the western Himalayas*, Geological Society of America, special paper 232, p. 75-94

Kushiro, I. & Yoder, H.S., 1966, Anorthite-fosterite and anorthite-enstatite relations and their bearing on the basalt-eclogite transformation, *Journal of Petrology*, v. 7, p. 337-362.

Kusky, T.M., Lu, W., Dilek, Y., Robinson, P., SongBai, P. & XuYa, H., 2011, Application of the modern ophiolite concept with special reference to Precambrian ophiolites, *Science China Earth Sciences*, v. 54, p. 315-341.

Legato, J.M., 1986, The *geology of the Heardmont quadrangle, Georgia-South Caroline*, unpublished M.S. thesis, University of Georgia, Athens, 144 p.

Lipin, B.R., 1984, Chromite from the Blue Ridge province of North Carolina, *American Journal of Science*, v. 284, p. 507-529.

Maier, W.D., Arndt, N.T. & Curl, E.A., 2000, Progressive crustal contamination of the Bushveld Complex: evidence from Nd isotope analyses of the cumulate rocks, *Contributions to Mineralogy and Petrology*, volume 140, p. 316-227.

Malpas, J., 1978, Magma generation in the upper mantle, field evidence from ophiolite suites, and application to the generation of oceanic lithosphere, *Philosophical Transaction of the Royal Society of London*, v. 288 A, p. 527-546.

McFarland, T.L., 1992, *Geochemical and petrographic study of the Russell Lake Allochthon in north-east Georgia*, Unpublished M.S. thesis, University of Georgia, Athens, 315 p.

McSween, H.Y., Jr., Sando, T.W., Clark, S.R., Harden, T.J. & Strange, E.A., 1984, The gabbro-metagabbro association of the Southern Appalachian Piedmont, *American Journal of Science*, v. 284, p. 437-461.

Metcalf, R.V., and Shervais, J.W., 2008. Supra-Subduction Zone (SSZ) Ophiolites: Is there really an "ophiolite conundrum"?, in J.E. Wright and J.W. Shervais (eds.), *Ophiolites, arcs, and batholiths: A tribute to Cliff Hopson,* Geological Society of America Special Paper **438**, p. 191–222.

Misra, K.C. & Keller, F.B., 1978, Ultramafic bodies in the

southern Appalachians: a review, *American Journal of Science*, v. 278, p. 389-418.

Miller, D.J. & Christensen, N.I., 1994, Seismic signature and geochemistry of an island arc: a multidisciplinary study of the Kohistan accreted terrane, northern Pakistan, *Journal of Geophysical Research*, v. 99, no. B6, p. 11623-11642.

Mittwede, S.K., 1989, The Hammett Grove Meta-igneous Suite; a possible ophiolite in the northwestern South Carolina Piedmont, in: S.K. Mittwede and E.F. Stoddard (eds), *Ultramafic Rocks of the Appalachian Piedmont*, Geological Society of America, Special Paper 231, p. 45-62.

Niu, Y. & O'Hara, M.J., 2008, Global correlations of ocean ridge basalt chemistry with axial depth: a new perspective, *Journal of Petrology*, v. 49, p. 633-664.

Norrish, K. & Hutton, J.T., 1969, An accurate x-ray spectrographic method for the analyses of a wide range of geological samples, *Geochimica et Cosmochimica Acta*, v. 33, p. 431-453.

Owens, B.E. & Uschner, N.E., 2001, Mineralogy and geochemistry of metamorphosed ultramafic rocks in the central Piedmont Province of Virginia, *Southeastern Geology*, v. 40, p. 213-229.

Paster, T.P., Schauwecker, D.S. & Haskin, L.A., 1974, The behaviour of some trace elements during the solidification of the Skaergaard layered series, *Geochimica et Cosmochimica Acta*, v. 38, p. 1549-1577.

Pavlides, L., 1981, *The central Virginia volcanic-plutonic belt: an island arc of Cambrian(?) age*, US Geological Survey, Professional Paper 1231-A, Washington, DC, 34 p.

Pearce, J.A., 1983, Role of the subcontinental lithosphere in magma genesis at active continental margins, in: Hawkesworth, C.J. and Norry, M.J. (eds.), *Continental basalts and mantle xenoliths*, Shiva, Nantwich, pp. 230-249.

Pearce, J.A., Lippard, S.J., and Roberts, S., 1984, Characteristics and tectonic significance of supra-subduction zone ophiolites, *in* Kokelaar, B.P., and Howells, M.F., eds., *Marginal Basin Geology*, California, Blackwell Scientific Publications, Palo Alto, p. 74–94.

Peterson, V. & Ryan, J.G., 2009, Petrogenesis and structure of the Buck Creek mafic-ultramafic suite, southern Appalachians: constrains on ophiolite evolution and emplacement in collisional orogens, Geological Society of America Bulletin, v. 121, p. 615-629.

Petterson, M., G., 2010, A review of the geology and tectonics of the Kohistan island arc, north Pakistan, in: Kusky, T.M., Zhai, M.-G. & Xiao, W. (eds.), *The evolving continents: understanding processes of continental growth*, Geological Society of London, Special Publication no. 338, p. 287-327.

Raymond, L.A., Swanson, S.E., Love, A.B. & Allan, J.F., 2003, Cr-spinel compositions, metadunite petrology, and the petrotectonic history of Blue Ridge ophiolites, southern Appalachian orogen, USA, In: Y. Dilek & P.T. Robinson (eds.), *Ophiolites in Earth History*, Geological Society of London, Special Publication 218, p. 253-278.

Rollinson, H.R., 1993, *Using geochemical data: evaluation, presentation, interpretation*, John Wiley and Sons, New York, 352 p.

Schilling, J-G., Zajac, M., Evans, R., Johnston, T, White, W., Devine, J.D. & Kingsley, R., 1983, Petrologic and geochemical variations along the Mid-Atlantic Ridge from 29°N to 73°N, *American Journal of Science*, v. 283, p. 510-586.

Schuth, S., Munker, C., Konig, S., Qopoto, C., Basi, S., Gabre-Schonberg, D. and Ballhaus, C., 2009, Petrogenesis of Lavas along the Solomon Island Arc, SW Pacific: Coupling of compositional variations and subduction zone geometry, *Journal of Petrology*, v. 50, p. 781-811.

Secor, D.T., Jr., Snoke, A.W. & Dallmeyer, R.D., 1986, Character of the Alleghanian orogeny in the Southern Appalachians, Part III. Regional relationships, *Geological Society of America Bulletin*, v. 97, p. 1345-1353.

Shaw, H.F. & Wasserburg, G.J., 1984, Isotopic constrains on the origin of Appalachian mafic complexes, *American journal of Science*, v. 284, p. 319-349.

Shervais, J.W., 2001, Birth, death, and resurrection: The life cycle of suprasubduction zone ophiolites, *Geochemistry, Geophysics, Geosystems*, v. 2, doi: 10.1029/2000GC000080.

Sisson, T.W. and Layne, G.D., 1993, H_2O in basalt and basaltic andesite glass inclusions from four subduction-related volcanoes, *Earth & Planetary Science Letters*, v. 117, p. 619-635.

Stanley, R.S., Roy, D.L., Hatch, Jr., N.L. & Knapp, D.A., 1984, Evidence for tectonic emplacement of ultramafic and associated rocks in the pre-Silurian eugeosynclinal belt of western New England – vestiges of an ancient accretionary wedge, *American Journal of Science*, v. 284, p. 559-595.

Stoddard, E.F., Kite, L.E. & Moye, R.J., 1982, Ophiolite terranes of the eastern Piedmont of North Carolina and their tectonic implications: *Geological Society of America, Program with Abstracts*, Northeastern and Southeastern Meeting, v. 14, p. 86.

Streckeisen, A., 1976, To each plutonic rock its proper name, *Earth Science Reviews*, v. 12, p. 1-33.

Sun, S.-S., and McDonough, W.F., 1989, Chemical and isotopic systematics of oceanic basalts: Implications for mantle composition and processes, *in* Saunders, A.D., and Norry, M.J., eds., Magmatism in the Ocean Basins: Geological Society [London] Special Publication 42, p. 313–345.

Swanson, S.E., 2001, Ultramafic rocks of the Spruce Pine area, western North Carolina: a sensitive guide to fluid migration and metamorphism, *Southeastern Geology*, v. 40, p. 163-182.

Swanson, S.E., Raymond, L.A., Warner, R.D., Ryan, J.G., Yurkovich, S.P. & Peterson, V.L., 2005, Petrotectonics of mafic and ultramafic rocks in the Blue ridge terranes of western North Carolina and northeast Georgia, in:

R.D. Hatcher, Jr. & A.J. Mershat (eds.), *Blue ridge geology geotraverse east of the Great Smoky Mountains National Park, Western North Carolina*, North Carolina Geological Survey, Carolina Geological Society, 2005 Annual Fieldtrip Guidebook, p. 73-90.

Tenthorey, E.A., Ryan, J.G. & Snow, E.A., 1996, Petrogenesis of sapphirine-bearing metatroctolites from the Buck Creek ultramafic body, southern Appalachians, *Journal of Metamorphic Geology*, v. 14, p. 103-114.

Thornber, C.R., 1981, Olivine-liquid relations of lava erupted by Kilauea volcano from 1994 to 1998: implications for shallow magmatic processes associated with the ongoing East-Rift-Zone eruption, *Canadian Mineralogist*, v. 39, p. 239-266.

Thornber, C.R., Budahn, J.R., Ridley, W.I. & Unruh, D.M., 2003, Trace element and Nd, Sr, Pb isotope geochemistry of Kilauea volcano, Hawaii, near-vent eruptive, *U.S. Geological Survey, Open File Report 03-493*, 5p.

Tomilenko, A.A. & Kovyazin, S.V., 2008, Development of corona textures around olivine in anorthosites of the Korosten' pluton, Ukrainian shield: mineralogy, geochemistry, and fluid inclusions, *Petrology*, v. 16, p. 87-103

Walker, J.A., Roggensack, K., Patino, L.C., Cameron, B.I. and Matias, O., 2003, The water and trace element contents of melt inclusions across an active subduction zone, *Contribution to Mineralogy and Petrology*, v. 146, 62-77.

Warner, R.D., 2001, Mineralogy and petrology of metaultramafic rocks at Buck Creek, North Carolina, *Southeastern Geology*, v. 40, p. 183-200.

West, H.B., Garcia, M.O., Gerlach, D.C. & Romano, J., 1992, Geochemistry of tholeiites from Lanai, Hawaii, *Contributions to Mineralogy & Petrology*, v. 112, p. 520-542.

Whitney, J.A., Herz, N. & Legato, J.M., 1987, Allochthonous mafic and ultramafic lithologies from near the Russell Lake reservoir, eastern Georgia: evidence for late Proterozoic thrust emplacement of a dismembered ophiolite, *Geological Society of America Abstracts with Programs*, v. 19, p. 136.

SOUTHEASTERN GEOLOGY
V. 49, No. 2, October 2012, p.79-90

HOLOCENE BEACHROCK IN THE DRY TORTUGAS, FLORIDA, U.S.A.

CARL R. FROEDE JR.

U.S. Environmental Protection Agency, Region 4,
61 Forsyth St.
Atlanta, Georgia 30303-8960, USA

EUGENE A. SHINN

The College of Marine Science
University of South Florida
140 Seventh Ave., South
University of South Florida
St. Petersburg, Florida 33701, USA

ABSTRACT

The Dry Tortugas contain beachrock of Holocene age. It is generally composed of biogenic and detrital sedimentary, sand-sized carbonate particles cemented by interstitial aragonite precipitation. These lithified deposits occur adjacent to and/or in close proximity to several islands (i.e., Keys) in intertidal and presently shallow subtidal environments. An investigation was conducted and beachrock is reported where visually identified. Its location and form suggest that it can aid in understanding changes to island morphology that occurred during the Holocene.

INTRODUCTION

The Spanish explorer Ponce de León first identified the islands comprising Las Tortugas (The Turtles) in 1513 (National Park Service [NPS], 2010). In 1819, the United States acquired Florida from Spain and the Dry Tortugas became part of the Florida Territory (Unger, 1992). Garden Key became the most developed of the islands with the construction of a lighthouse initiated in 1824, followed by the construction of Fort Jefferson beginning in 1846 (NPS, 2011). Focused scientific investigation of the biology, ecology, and to a lesser extent the geology of the Dry Tortugas and Florida Keys began following the establishment of the Carnegie Dry Tortugas Laboratory for Marine Ecology on Loggerhead Key in 1905 (Figure 1).

Beachrock outcrops on Loggerhead Key attracted the attention of some of the laboratory's early visitors. Subsequent investigation identified beachrock in an intertidal and/or shallow subtidal, shore-parallel setting at several islands. Where present, this unique lithotype can aide in defining geomorphic changes to islands in the Dry Tortugas. An aerial and ground-based reconnaissance was undertaken to determine the presence, extent, and occurrence of beachrock at each of the seven islands in the Dry Tortugas.

BEACHROCK: AN OVERVIEW

Sir Francis Beauford first reported beachrock along the southern coast of Asia Minor (i.e., modern Turkey) in 1817 (Goudie, 1969). It has subsequently been identified in numerous diverse tropical to temperate, marine to freshwater environments (see extensive reviews in Gischler, 2007, and Vousdoukas and others, 2007). Beachrock has been attributed to four different processes: 1) direct calcium carbonate precipitation from solution, 2) precipitation by mixing of marine and meteoric water, 3) carbon dioxide de-gassing of calcium carbonate in solution, and 4) cement precipitation through biological activity. This variability illustrates the complexity surrounding beachrock development and its apparent location-specific mode of formation. The cementing agent occurs as interstitial aragonite and/or high magnesium calcite (Stoddart and Cann, 1965; Land, 1970; Bricker,

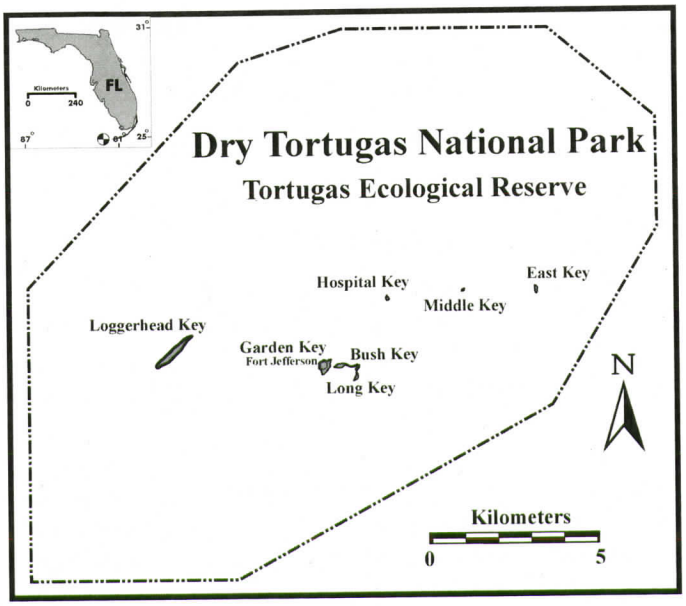

Figure 1. Dry Tortugas National Park/Tortugas Ecological Reserve is located approximately 113 km west of Key West, Florida, and covers an area of approximately 11,914 hectares. The park forms the westernmost portion of the Florida Keys National Marine Sanctuary and contains a cluster of seven islands (i.e., Keys). The individual Keys are composed predominately of coral debris and carbonate sand derived from various biological organisms.

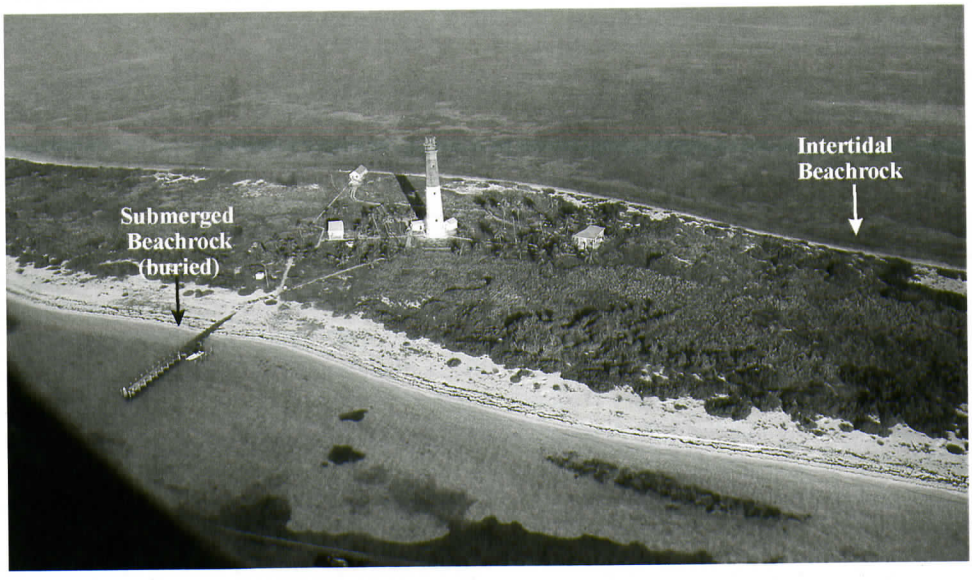

Figure 2. Aerial image (looking west; altitude ~152 m) across the central portion of Loggerhead Key showing the location of submerged beachrock (covered by sediments at the time of our 2011 investigation) and exposed intertidal beachrock. The island is approximately 1,250 m in length by 220 m in width. Photograph from September 2011.

Figure 3. A portion of pipe extends out of beachrock located on the northwestern side of Loggerhead Key. The pipe was part of the infrastructure supporting the Carnegie Dry Tortugas Laboratory for Marine Ecology constructed in 1905. The formation of beachrock subsequent to pipe installation cemented it in place. Shoreline erosion has exposed the pipe in the surf zone. Scale in centimeters and inches. Photograph from October 2005.

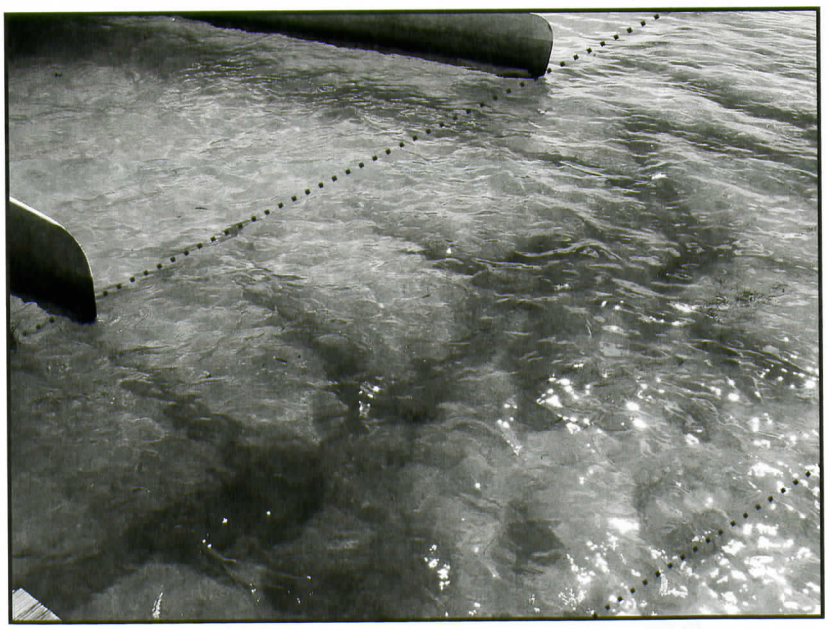

Figure 4. Subtidal beachrock became exposed adjacent to the shore at the pier on Loggerhead Key (see Figure 2) following Hurricane Katrina. The weathered, rectangular-jointed outcrop is approximately three to four meters wide and within the diagonal lines of black dots (see also Shinn, 2009, his Figure 5). Photograph from October 2005.

Figure 5. Intertidal beachrock exposed at low tide along the northwestern shoreline on Loggerhead Key. Looking southwest. Photograph from October 2005.

1971; Scoffin and Stoddart, 1983; Guo and Friedman, 1990). Once beachrock has formed, the shoreline is armored and only intense storm waves coupled with the undermining of the unlithified underlying sediments appear capable of removing its protection (Bain, 1988; Cooper, 1991; Dickinson, 1999).

Beachrock development varies from less than a year to several years (Daly, 1924; Emery and others, 1954; Frankel, 1968; Scoffin, 1970; Schmalz, 1971; Easton, 1974; Scoffin and Stoddart, 1983; Chivas and others, 1986; Shinn, 2011). Age determination via radiometric dating can yield unreliable results if derived from the various detrital or biogenic sedimentary particles (McLean and others, 1978; Scoffin and Stoddart, 1983; Hopley, 1986). A more reliable age can be determined if the actual cement is used. More recently, oxygen isotopes in beachrock have been used to decipher past climate history (Friedman, 2004, 2005). Beachrock is not limited to the intertidal zone or foreshore but can extend landward within the shallow subsurface (Daly, 1924; Russell, 1962, 1963; Alexandersson, 1972; Moore, 1977; Higgins, 1968; Gischler, 2007; Vousdoukas and others, 2007). This variability may create problems when attempting to pinpoint a former shoreline position. Once exposed, beachrock undergoes erosion through three different processes: 1) mechanical erosion, 2) biological erosion, and 3) chemical erosion (Revelle and Emery, 1957; Scoffin and Stoddart, 1983). Its durability has not been investigated in detail and could prove to be a fruitful area of further research.

Beachrock has been used as a sea level indicator (see review in Gischler, 2007); however, its variability in development has raised concerns regarding possible misinterpretation (Stoddart and Cann, 1965; Scoffin and Stoddart, 1983; Hopley, 1986; Kelletat, 1988, 2006). Its occurrence suggests that beachrock could be useful in island morphological studies.

BEACHROCK SURVEYS OF THE DRY TORTUGAS

The carbonate sand forming the islands in the Tortugas is composed of particles of coral,

Halimeda, bryozoan, molluscan shells, echinoderms, foraminifera, and coralline algae fragments (Multer, 1971; Shinn and Jaap, 2011). The carbonate cement binding these materials into beachrock has been identified as aragonite (Daly, 1924; Ginsburg, 1953; Multer, 1971). The beachrock in the Tortugas is interpreted as Holocene deposits due to its location along the shoreline and adjacent shallow subtidal settings (Multer, 1971; Shinn, 2009).

Loggerhead Key

The Carnegie Dry Tortugas Laboratory for Marine Ecology was established on Loggerhead Key by Alfred G. Mayor in 1905 (Colin, 1980; Stephens and Calder, 2006; NPS, 2007; Shinn and Jaap, 2011). Despite its primary focus on the study of tropical marine life and ecology, exposures of beachrock on Loggerhead Key attracted the attention of some of its early visitors (Figure 2). Vaughn (1914) was the first to report on beachrock and he postulated that wave agitation formed the exposures on both sides of the island. He noted that the rock sloped seaward and believed that Loggerhead Key was a wave-built island. Vaughn also postulated that the beachrock was approximately 2.4 m in thickness, but subsequent investigation has determined it to be no more than one meter thick (Shinn and Jaap, 2011). Mayor invited Harvard coworker Richard Field to visit the Tortugas and assess the conditions of beachrock development. Field (1919, 1920) suggested that carbonate saturated groundwater discharged through the beach sands along the shoreline between tides. Cement precipitated in the interstitial pore spaces due to pressure release and the escape of carbon dioxide, lowering the solubility of the calcium carbonate. Daly (1920) was also invited by Mayor to investigate the beachrock exposures on the island. He initiated a field experiment to determine if the breakdown of organic matter within the carbonate materials would generate calcite cement that could precipitate along the shoreline between tides. Unfortunately, a hurricane in 1919 destroyed that experiment.

Daly (1924) reported that Mayor had observed the rapid incorporation of newly deposited sediments into beachrock following a hurricane in 1910. Daly (1924) subsequently completed his microscopic assessment of beachrock from Loggerhead Key while on American Samoa and concluded that the cementing agent was needle-shaped aragonite crystals. He envisioned a complex means of carbonate precipitation initiated with the accumulation of littoral beach sand provided by major storms. The putrefaction of organic materials (including bacteria) within the sands, combined with heat and differential air pressure within the interstitial pore spaces to produce carbonate cement that formed beachrock.

In 1937, Lecompte noted the rapid formation of beachrock on the island as it had incorporated bricks, bottles, and other modern debris (Figure 3). Regarding beachrock removal, he hypothesized that a combination of dissolution and mechanical grinding by coral or shell particles created excavations and enhanced erosion. Ginsburg (1953) conducted an extensive petrographic investigation of beachrock on Loggerhead Key. He attributed beachrock cement formation to the influence of increasing temperatures and rapid water drainage within the intertidal zone. Multer (1971) however, thought that the lack of groundwater coupled with no evidence of any sand-grain dissolution, suggested that cement formed due to alternating wet-dry cycles of sea spray on littoral beach sands that triggered aragonite precipitation from a supersaturated calcium carbonate solution. More recently, Shinn (2009) proposed that beachrock forms from wave/tidal pumping of seawater into the beach sand along the shoreline coupled with high evaporation of the discharging carbonate-rich fluids between tides. He also explained how subtidal beachrock exhibiting rectilinear jointing could be incorrectly interpreted as the anthropogenic remains of long lost civilizations (e.g., Atlantis; Figure 4) [Harrison, 1971; Shinn, 1978, 2004; McKusick and Shinn, 1980]. The development of beachrock on the northwestern side of the island has likely preserved it from erosion due to passing storms and hurricanes (Figure 5). The subtidal outcrop of beachrock on the southeastern side of the island

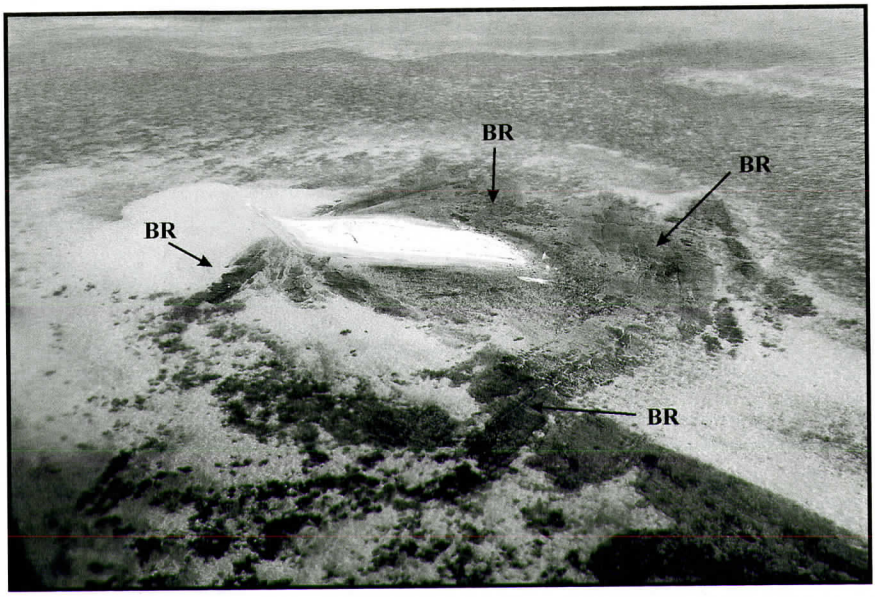

Figure 6. An aerial image (altitude ~152 m) looking toward the north-northwest across Hospital Key. Today, the island (white area slightly off center) is approximately 65 meters in length by 25 meters in width. The prominent subtidal beachrock (BR) surrounding the small island reflects its former size and likely higher elevation. Photograph from September 2011.

has also helped maintain and preserve this portion of the island.

Hospital Key

Sand Key was renamed Hospital Key following the construction of a small wooden building used as a hospital and for yellow-fever quarantine in the 1860s (Shinn and others, 1989; Shinn and Jaap, 2011). The hospital structure and its brick and mortar foundation were subsequently destroyed by a hurricane. Storm waves and occasional washover events have greatly diminished the size of the island. Subtidal beachrock has been reported in two to three meters of water just south of the island (Shinn and Jaap, 2011). Our aerial survey indicates that beachrock is far more extensive, actually surrounding the island (Figure 6).

Middle Key

Beachrock has not been reported at this island, and none was observed in the aerial survey in September 2011 (Figure 7). Likely, its small size and frequent inundation prevent conditions necessary for beachrock development. The absence of beachrock, both within the intertidal zone or submerged offshore surrounding the island, suggests that either it has been too small to form beachrock or conditions were not conducive for its formation if the island was larger in the past.

East Key

Davis and O'Neill (1979) reported that during the American Civil War beachrock was identified on the island, but they were unable to locate any exposures in their study of East Key. Our aerial assessment of East Key also failed to identify any beachrock exposures either adjacent to the shoreline or offshore from the island (Figure 8).

Long Key

Today, a thin ribbon of sand connects Long Key and Bush Key. However, they will be reviewed separately. Geomorphologically,

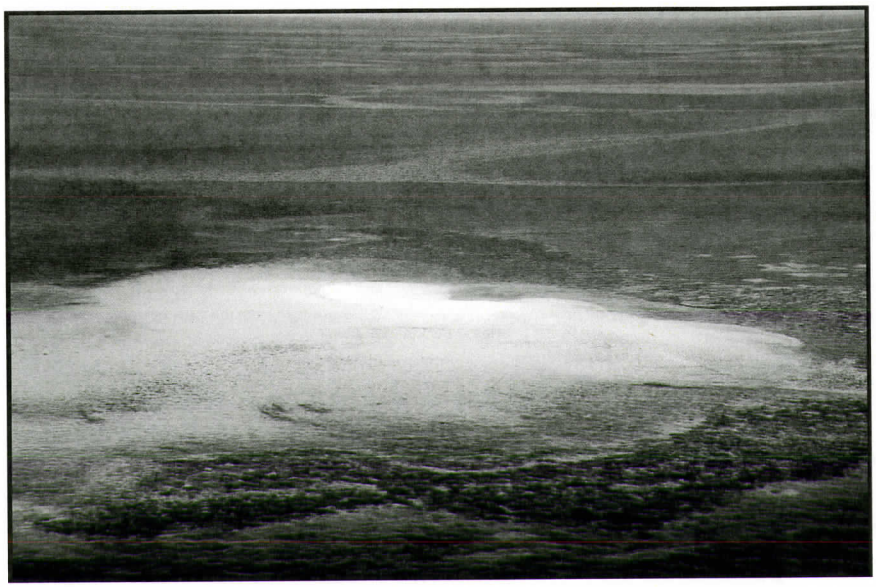

Figure 7. Middle Key is intermittently exposed due to seasonal variations in waves and tides. No beachrock was observed nor has any been reported for this locale. The island is approximately 45 meters in length and no more than 10 meters in width. The view is looking toward the north (altitude ~152 m). Photograph from September 2011.

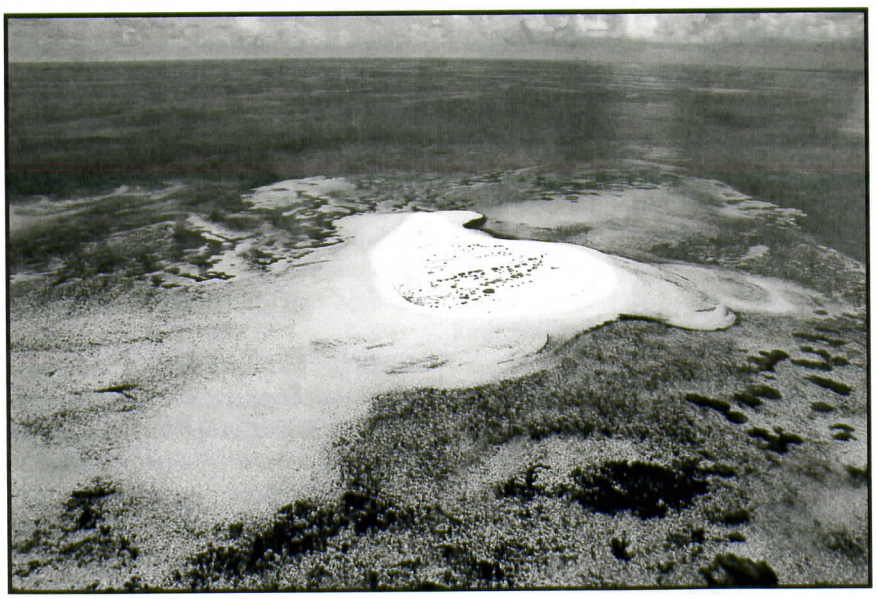

Figure 8. Looking toward the north, East Key is approximately 175 meters at its widest point (altitude ~152 m). While beachrock has been reported at this locale none was observed in the aerial flyover on September 2011.

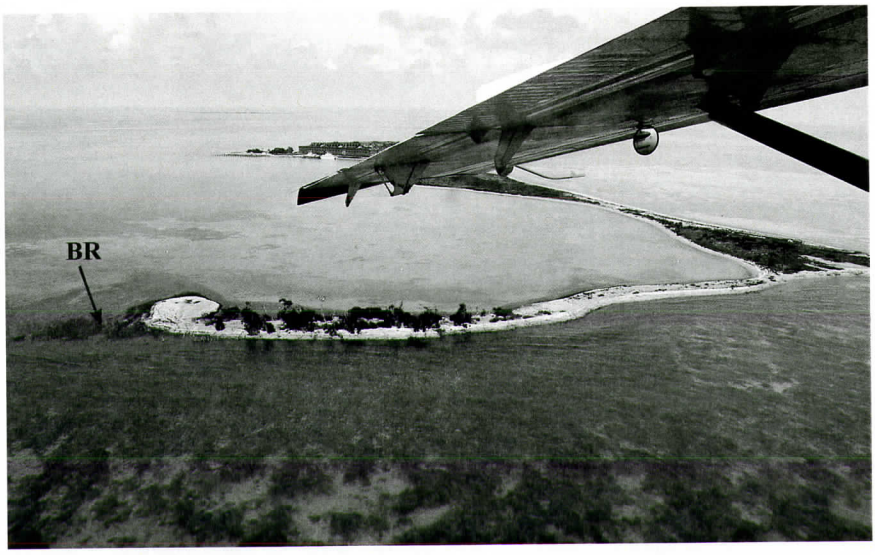

Figure 9. Looking toward the west (altitude ~152 m), Long Key lies in the foreground and parallel to the horizon. An intertidal outcrop of beachrock (BR) is exposed along the southern shore of the island as indicated by the arrow. The island is approximately 310 meters in length and no more than 36 meters in width. Photograph from September 2011.

beachrock should be expected at Long Key due to its size and extensive beach, but none has been reported. However, our aerial survey reveals that beachrock appears to be present in the intertidal zone along its southern shoreline (Figure 9). The outcrop resembles the beachrock exposed in the intertidal zone on Loggerhead Key. Presently, the island is off limits to the public (NPS, 2008) and field verification remains to be conducted.

Bush Key

No beachrock has been reported within the intertidal or subtidal zones at Bush Key. However, the geomorphology of the island suggests that beachrock may be present and further investigation of the island shoreline and offshore waters is warranted (Figure 10).

Garden Key

A lighthouse was built on Garden Key between 1824 and 1826. Construction of Fort Jefferson was begun in 1846, but stopped in 1875 with the fortress still unfinished (NPS, 2011). The brick and mortar fort rests on unconsolidated carbonate sand. Vertical fracturing began in some of the walls soon after construction stopped due to uneven settling. In 2005, the U.S. Geological Survey drilled seven wells on Garden Key (Figure 11). The wells were cored to the Pleistocene limestone (average depth 16.8 m) and Holocene beachrock was not encountered in any well. Our aerial survey and ground-based exploration of Garden Key did not reveal any beachrock on or adjacent to the island.

CONCLUSIONS

Holocene beachrock found in the Tortugas, especially at Loggerhead Key, has provided an exceptional locale in which to study this interesting process and resultant landform. Many modern theories of beachrock formation are consistent with past observations made at Loggerhead Key. The first petrographic studies of beachrock were conducted on materials collected on this island.

The origin of beachrock remains site specific as its rate and style of formation, development, and preservation can vary from one locale to the next. Apparently, no single model can account

Figure 10. Looking toward the southwest with Bush Key in the foreground and Garden Key (largely contained by antebellum Fort Jefferson) in the background (altitude ~152 m). Beachrock has not been reported at either island, but Bush Key appears to be geomorphologically conducive to beachrock development. Bush Key is approximately 735 meters in length and no more than 157 meters at its widest point (in background). Photograph from September 2011.

for its origin from varied physical conditions such as marine or freshwater environments and areas having tropical or temperate climates. That beachrock can develop rapidly suggests that it may form where it was previously unidentified based on changing environmental conditions. The only common factor in beachrock formation is that individual sedimentary grains must remain in contact with each other long enough for aragonite/carbonate cement to precipitate interstitially and bind the grains together.

Past investigation of the Dry Tortugas identified beachrock at several Keys. However, the dynamic changes to the islands over the years may have either eroded the beachrock or covered it. We verified its presence at known locales (e.g., Loggerhead Key and Hospital Key) and identified a new exposure at Long Key. Bush Key may well support beachrock development and further investigation of that island and the adjacent area offshore is necessary.

The presence of beachrock indicates it may serve as a means of understanding past island morphology. Found subtidally around Hospital Key, suggests that the island was formerly larger and higher in elevation than today. Erosion has undermined the unlithified sediments beneath the beachrock causing it to subside below the water surface as the island retreated from its former position (see Shinn, 2009). The intertidal beachrock on the southern end of Long Key could prove beneficial in defining the former southern extent of that island. Radiometric dating of the interstitial carbonate cements could supply valuable data useful in documenting the former age and size of the islands. Our assessment of beachrock in the Tortugas suggests that more should be found and further study into the age and past morphology of the Keys is warranted.

ACKNOWLEDGMENTS

We are appreciative to P. Vierheller and K. Piselli for their reference assistance. Gratitude is expressed to A.J. Akridge, J.K. Reed, K. Rasmussen, and R.J. Wilber for their helpful and constructive comments. For Mr. Froede, this work neither represents the views or opinions of

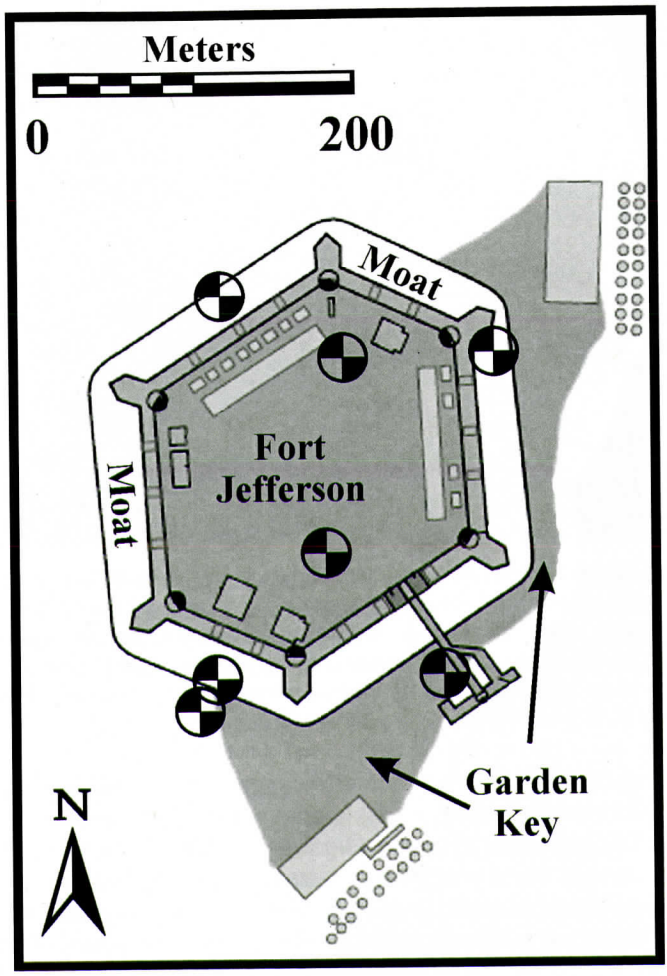

Figure 11. Garden Key is dominated by Fort Jefferson. A moat surrounds the fort. Seven wells (circular panels) were drilled and cored by the U.S. Geological Survey on the island. No Holocene beachrock was identified in the subsurface. Modified National Park Service map.

the U.S. Environmental Protection Agency or the United States, nor was this investigation conducted in any official capacity. Dr. Shinn is grateful for the friendship and support from colleagues D.W. Griffin, T.D. Hickey, and A.B. Tihansky, and their work with him on coring Garden Key. Any mistakes are the responsibility of the authors.

REFERENCES CITED

Alexandersson, T., 1972, Mediterranean beachrock cementation: Marine precipitation of Mg-Calcite, in Stanley, D.J., ed., The Mediterranean Sea: A Natural Sedimentation Laboratory: Stroudsburg, Pennsylvania, Dowden, Hutchinson, and Ross, p. 203-223.

Bain, R.J., 1988, Exposed beachrock: Its influence on beach processes and criteria for recognition, *in* Mylroie, J.E., ed., Proceedings of the 4th Symposium on geology of the Bahamas: San Salvador, Bahamas, Bahamian Field Station, p. 33-44.

Bricker, O.P., 1971, Introduction: Beachrock and intertidal cement, *in* Bricker, O.P., ed., Carbonate Cements: Baltimore, Maryland, Johns Hopkins Press, p. 1–13.

Chivas, A., Chappell, J., Polach, H., Pillans, B., and Flood, P., 1986, Radiocarbon evidence for the timing and rate of island development, beach-rock formation and phosphatization at Lady Elliot Island, Queensland, Australia: Marine Geology, v. 69, p. 273–287.

Colin, P. L., 1980, A brief history of the Tortugas Marine

Laboratory and the Department of Marine Biology, Carnegie Institutions of Washington, *in* Sears, M., and Merriam, D., eds., Oceanography: The Past: New York, Springer-Verlag, p. 138-147.

Cooper, J.A.G., 1991, Beachrock formation in low latitudes: Implications for coastal evolutionary models: Marine Geology, v. 98, p. 145-154.

Daly, R.A., 1920, Origin of beach-rock: Carnegie Institution of Washington Year Book, v. 18, p. 192.

Daly, R.A., 1924, The geology of American Samoa: Carnegie Institution of Washington Publication 340, p. 93-143.

Davis, R.A., Jr., and O'Neill, C.W., 1979, Morphodynamics of East Key, Dry Tortugas, Florida, *in* Halley, R.B., ed., Guide to sedimentation for the Dry Tortugas: Tallahassee, Florida, Southeastern Geological Society, Publication 21, p. 7-14.

Dickinson, W.R., 1999, Holocene sea-level record on Funafuti and potential impact of global warming on central Pacific atolls: Quaternary Research, v. 51, p. 124-132.

Easton, W.H., 1974, An unusual inclusion in beachrock: Journal of Sedimentary Petrology, v. 44, p. 693–694.

Emery, K.O., Tracey, J.I., Jr., and Ladd, H.S., 1954, Geology of Bikini and nearby atolls: Washington, D.C., U.S. Geologic Survey Professional Paper 260-A, 265 p.

Field, R. M., 1919, Investigations regarding the calcium carbonate oozes at Tortugas, and the beach-rock at Loggerhead Key: Carnegie Institution of Washington Year Book, v. 18, p. 197-98.

Field, R. M., 1920, Origin of "beachrock" (coquina) at Loggerhead Key, Tortugas (abs.): Bulletin of the Geological Society of America, v. 31, p. 215.

Frankel, E., 1968, Rate of formation of beach rock: Earth and Planetary Science Letters, v.4, p. 439-440.

Friedman, G.M., 2004, Holocene chronostratigraphic beachrocks and their geologic climatic significance, *in* Hill, R.J., Leventhal, J., Aizenshtat, Z., Baedecker, M.J., Claypool, G., Eganhouse, R., Goldhaber, M., and Peters, K., eds., Geochemical Investigations in Earth and Space Science—A Tribute to Isaac R. Kaplan: New York, Elsevier, p. 125-142.

Friedman, G.M., 2005, Climatic significance of Holocene beachrock sites along shorelines of the Red Sea: American Association of Petroleum Geologists Bulletin, v. 89, p. 849-852.

Gischler, E., 2007, Beachrock and intertidal precipitates, *in* Nash, D.J., and McLaren, S.J., eds., Geochemical sediments and landscapes: Oxford, United Kingdom, Blackwell Scientific, p. 365-390.

Ginsburg, R.N., 1953, Beachrock in south Florida: Journal of Sedimentary Petrology, v. 23, p. 85-92.

Goudie, A., 1969, A note on Mediterranean beachrock: Its history: Atoll Research Bulletin, v.126, n.19, p. 11–14.

Guo, B., and Friedman, G.M., 1990, Petrophysical characteristics of Holocene beachrock: Carbonates and Evaporites, v. 5, p. 223-243.

Harrison, W., 1971, Atlantis undiscovered—Bimini, Bahamas: Nature, v. 230, p. 287-289.

Higgins, C.G., 1968, Beachrock, *in* Fairbridge, R.W., ed., Encyclopedia of Geomorphology: New York, Reinhold, p. 70-73.

Hopley, D., 1986, Beachrock as a sea-level indicator, *in* van de Plassche, O., ed., Sea-level Research: A Manual for the Collection and Evaluation of Data: Norwich, United Kingdom, Geo Books, p. 157-173.

Kelletat, D., 1988, Zonality of modern coastal processes and sea-level indicators: Palaeogeography, Palaeoclimatology, Palaeoecology, v. 68, p. 219-230.

Kelletat, D., 2006, Beachrock as sea-level indicator? Remarks from a geomorphological point of view: Journal of Coastal Research, v. 22, p. 1558-1564.

Land, L.S., 1970, Phreatic versus vadose meteoric diagenesis of limestones: Evidence from a fossil water table: Sedimentology, v. 14, p. 175-185.

Lecompte, M., 1937, Some observations on the coral reef area of Tortugas: Carnegie Institution of Washington Year Book, v. 36, p. 96-97.

McKusick, M., and Shinn, E.A., 1980, Bahamian Atlantis reconsidered: Nature, v. 287, p. 11-12.

McLean, R.F., Stoddart, D.R., Hopley, D., and Polach, H., 1978, Sea level change in the Holocene on the northern Great Barrier Reef: Philosophical Transactions of the Royal Society of London, v. A-291, p. 167-186.

Moore, C.H., Jr., 1977, Beach rock origin: Some geochemical, mineralogical, and petrographic considerations: Geoscience and Man, v. XVIII, p. 155-163.

Multer, H.G., 1971, Holocene cementation of skeletal grains into beachrock, Dry Tortugas, *in* Bricker, O.P., ed., Carbonate cements: Baltimore, Maryland, Johns Hopkins Press, p. 25-26.

NPS, 2007, Life on Loggerhead brochure, Dry Tortugas National Park: Washington, D.C., U.S. Department of the Interior.

NPS, 2008, Code of Federal Regulations, Title 36, Chapter I, Compendium of Designations, Closures, Requests Requirements and Other Restrictions imposed under the discretionary authority of the Superintendent, Everglades and Dry Tortugas National Parks: Accessed from: http://www.nps.gov/drto/parkmgmt/upload/DRTO%20compendium%202008_final_.pdf, on 10/29/11.

NPS, 2010, Dry Tortugas National Park Brochure: Washington, D.C., U.S. Department of the Interior.

NPS, 2011, Dry Tortugas National Park website: http://www.nps.gov/drto/index.htm.

Revelle, R., and Emery, K.O., 1957, Chemical erosion of beach rock and exposed reef rock: Washington, D.C., U.S. Geological Survey Professional Paper 260-T, 21 p.

Russell, R.J., 1962, Origin of beach rock: Zeitschrift für Geomorphologie, v. 6, p. 1-16.

Russell, R.J., 1963, Beach rock: Journal of Tropical Geography, v. 17, p. 24-27.

Schmalz, R.F., 1971, Formation of beachrock at Eniwetok Atoll, *in* Bricker, O.P., ed., Carbonate Cements: Baltimore, Johns Hopkins Press, p. 17–24.

Scoffin, T.P., 1970, A conglomeratic beachrock in Bimini,

Bahamas: Journal of Sedimentary Petrology, v. 40, p. 756-758.

Scoffin, T.P., and Stoddart, D.R., 1983, Beachrock and intertidal cements, *in* Goudie, A.S., and Pye, K., eds., Chemical Sediments and Geomorphology: London, Academic Press, p. 401-425.

Shinn, E.A., 1978, Atlantis: Bimini hoax: Sea Frontiers, v. 24, p. 130–141.

Shinn, E.A., 2004, A geologist's adventures with Bimini beachrock and Atlantis true believers: Skeptical Inquirer, v. 28(1), p. 38–44.

Shinn, E.A., 2009, The mystique of beachrock, *in* Swart, P.K., Eberli, G.P., and McKenzie, J.A., eds., Perspectives in carbonate geology: A tribute to the career of Robert Nathan Ginsburg: Special Publication 41, International Association of Sedimentologists, Hoboken, New Jersey, Blackwell Publishing, p. 19-28.

Shinn, E.A., 2011, Interplay between Holocene sedimentation and diagenesis, and implications for hydrocarbon exploitation: Return to the sabkha of Ras Umm Said, Qatar, *in* Kendall. C.G.St., and Alsharhan, A., eds., Quaternary carbonate and evaporite sedimentary facies and their ancient analogues: A tribute to Douglas James Shearman: New York, Wiley-Blackwell, p. 133-148.

Shinn, E.A., and Jaap, W.C., 2011, Field guide to the major organisms and processes building reefs and islands of the Dry Tortugas: The Carnegie Dry Tortugas Laboratory Centennial Celebration (1905-2005): Tallahassee, Florida, Southeastern Geological Society Field Guide #54, 43 p.

Shinn, E.A., Lidz, B.H., Kindinger, J.L., Hudson, J.H., and Halley, R.B., 1989, A field guide: Reefs of Florida and the Dry Tortugas, *in* Hanshaw, P.M., ed., Sedimentation and stratigraphy of carbonate rock sequences, Volume 2: Washington, D.C., American Geophysical Union, p. T176:1-53.

Stephens, L.D., and Calder, D.R., 2006, Seafaring Scientist: Columbia, South Carolina, University of South Carolina Press, 220 p.

Stoddart, D.R., and Cann, J.R., 1965, Nature and origin of beach rock: Journal of Sedimentary Petrology, v. 35, p. 243-247.

Unger, F.A., 1992, Historical boundaries of Florida, *in* Fernald, E.A., and Purdum, E.D., eds., Atlas of Florida: Gainesville, Florida, University Press of Florida, p. 90.

Vaughan, T.W., 1914, The building of the Marquesas and Tortugas atolls and a sketch of the geologic history of the Florida Reef Tract: Carnegie Institution of Washington Publication 182, Papers of the Department of Marine Biology, v. 5, p. 55-67.

Vousdoukas, M.I., Velegrakis, A.F., and Plomaritis, T.A., 2007, Beachrock occurrence, characteristics, formation mechanisms and impacts: Earth-Science Reviews, v. 85, p. 23-46.

SOUTHEASTERN GEOLOGY
V. 49, No. 2, October 2012, p.91-94

REEXAMINATION OF EOCENE "GORCEIXITE" NODULES FROM ALABAMA AND SOUTH CAROLINA

HENRY BARWOOD

Department of Chemistry and Physics
Troy University
Troy, Alabama
hbarwood@troycable.net

ABSTRACT

Members of the crandallite group of minerals are found as nodules in the coastal plain of the southeastern United States. These nodules have been previously identified as the gorceixite member of the group. Recent analyses of nodules from Alabama and South Carolina show that they have a composition ranging from gorceixite (Ba dominant) to florencite (REE dominant). The source fluids for mineralization of these nodules is still uncertain.

INTRODUCTION

Complex nodules of crandallite group minerals are found discontinuously in Eocene sediments in Dale County, Alabama (near the town of Ariton) and in Aiken County, South Carolina. The nodules from Dale County are attributed to the early Eocene Bashi Marl, the basal member of the Hatchetigbee Formation within the Wilcox Group (Milton, et al., 1957).

Similar nodules from Aiken County in South Carolina are cited as being from the late Eocene Barnwell Group (Jackson Stage) (Michel, et al., 1982). While genetically similar, the nodules from Alabama and South Carolina are separated by a significant time interval and may represent paleosols developed on widespread unconformities developed within the Eocene sediments.

Nodules from both locations have been attributed to weathering of pyrite and organic enriched glauconitic sediments that created an acidic environment capable of leaching Barium and Rare Earth Elements (REE) that reacted with phosphate within the sediments to precipitate the crandallite group minerals. This origin is somewhat supported in Alabama by the presence of an erosional unconformity that removed the upper part of the Hatchetigbee in eastern Alabama (Szabo, et al., 1988).

The nodules incorporate sand grains from the enclosing sediments The presence of un-reacted monazite grains in specimens examined during this study argues against a purely weathering paragenesis for the nodules (Henry Barwood, personal communication). It is likely that the nodules are related to an Acid Phospho-Sulfate (APS) terrane developed during an unconformity, when pyrite-rich sediments were weathered (Dill, 2001; Dill, et al., 1995). The Barium, Strontium and REE could have been derived from volcanic ash incorporated into the overlying sedimentary layers.

All the nodules from Alabama and South Carolina were classified as gorceixite by the original investigators. Reexamination of specimens from these locations indicated that they might not be gorceixite and a subsequent investigation using Electron Probe Micro-Analysis (EPMA) was conducted.

SAMPLING LOCATIONS

The Dale County sites near the town of Ariton listed in Milton et al., 1957, were unavailable, having been built over or otherwise obliterated. In the mid-1970's a thick bed of "gorceixite" nodules was exposed 1 km west of the center of Ariton during development of a housing project. This location was sampled; however, samples are presently unavailable from this location. A field reconnaissance in 1996 revealed two existing locations where samples were collected for study. The first location, Ariton West, is a pasture where surface

Figure 1. Typical gorceixite nodule from the Ariton West location. The nodule is 6 x 5 cm in size. Nodules exceeding 20 cm have been found at this location. There are faint layers in the nodule that likely reflect the original bedding of the sediments. Weathering has reduced the enclosing sediments to a kaolinitic clay, which now encloses the nodules. Gorceixite nodules from all the Alabama and South Carolina localities are essentially identical in morphology to this specimen.

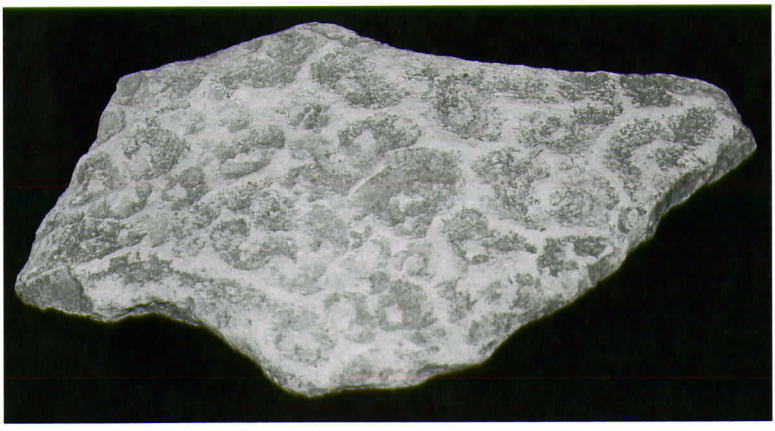

Figure 2. Gorceixite nodule from the Ariton East location. The nodules from this location are embedded in weathered shale and, like this specimen sometimes show diagenetic features. This specimen is 7 x 4 cm in size.

fragments of nodules are exposed by erosion (Figure 1). This site is located approximately 3 km west of the center of the town of Ariton, just south of highway 51. The second location, Ariton East, is in an overgrown roadcut on the south side of Highway 51, approximately 3 km east of the center of Ariton (Figure 2). The nodules here are in place.

The Aiken County, South Carolina sites roughly correspond to those listed in Ferguson, et al. 1979 and Michal, et al., 1982. They were re-examined in 1996 and, while the exact original locations were indeterminate, samples form the approximate location of these sites were re-

Table 1. Distribution of Ca, Ba, Sr, and REE from EPMA analysis.

Location	CaO	BaO	SrO	La_2O_3	Ce_2O_3	Pr_2O_3	Nd_2O_3	Sm_2O_3	Gd_2O_3	Y_2O_3	Sum REE
Ariton West	3.29	5.52	1.57	2.89	5.38	0.58	2.00	0.32	0.27	0.17	11.61
Ariton East	3.19	4.25	4.35	2.82	3.91	0.35	1.36	0.15	0.19	0.00	8.78
SC 1	0.52	22.16	1.63	0.25	0.31	0.05	0.21	0.05	0.18	0.09	1.14
SC 2	0.58	24.7	0.67	0.09	0.03	0.02	0.00	0.04	0.10	0.00	0.28
SC 3	1.09	12.2	1.78	1.82	4.42	0.57	2.37	0.35	0.24	0.00	9.77

Table 2. Raw data converted to the various molecules for the crandallite group. This showed that there was significant variation in the composition of the nodules, notably from those collected in Dale County, Alabama.

Sample Location	% Crandallite	% Gorceixite	% Goyazite	% Florencite	Sum
Ariton West	15.9	25.0	7.0	52.0	99.9
Ariton East	15.7	21.9	21.5	40.9	100.0
SC 1	2.0	87.1	6.4	2.5	98.0
SC 2	2.1	94.3	2.6	0.9	99.9
SC 3	4.4	49.1	7.2	39.4	100.1

sampled. None of the South Carolina samples were considered to be in place and were taken from road side ditches and road cuts. Sample SC1 was obtained from nodules exposed in a road cut along South Carolina State Highway 3104 approximately 2 km north of the community of Oakwood (locality 3 of Ferguson, et al.). Sample SC2 was obtained from a road cut along South Carolina State Highway 1669 approximately 4 km northeast of the community of Oakwood (locality 6 of Ferguson, et al.). Sample SC3 was collected in a bank exposed along Firetower Road approximately 2 km south of the community of Oakwood (locality 4 of Ferguson, et al.).

SAMPLE PREPARATION AND ANALYSIS

The nodule samples were embedded in epoxy resin in standard 25mm sample cups, ground and polished. The nodules range from compact to quite porous and it was difficult to obtain an adequate sample for analysis. Several mounts were prepared from each sample and the most homogenous was selected for analysis. After preparation, the samples were submitted to the University of Alabama EPMA lab where they were carbon coated and installed in the probe for analysis. The analysis was carried out on a Cameca SX-60 four channel microprobe. Standards and calibration were provided by the lab via an on-site technician. Once the EPMA was operational, control of the analytical phase was turned over to the operator for selection of beam size and location. All subsequent procedures were performed by the author.

The analytical routine used was called "crandallite" and analyzed for: Ca. Ba. Sr. La, Ce, Pr, Nd, Sm, Gd, Y, Al, Si, Ti, Fe, P, As, F and S. All output was reported as elemental values, and was converted to Oxides post-analysis. Interference from Ba and Ce L-alpha lines was resolved by cross-analyzing Ba and Ce standards and correcting for the line overlap (Bennett and Oliver 1992). This correction resulted in a 0.36 correction factor for Barium to Cerium.

ANALYTICAL RESULTS

The original research on these nodules indicated that, while considered gorceixite, there was some variability in composition, with the gorceixite molecule dominant. Analytical results from the EPMA data are presented in Table 1 (Oxide present) and Table 2 (Molecular percent). The recognized members of the crandallite group consist of:

Crandallite
$CaAl_3[(OH)_5(PO_4)_2]\cdot H_2O$

Gorceixite
$BaAl_3[(OH)_5(PO_4)_2]\cdot H_2O$

Goyazite
$SrAl_3[(OH)_5(PO_4)_2]\cdot H_2O$

Florencite –(Ce)
$(Ce,La,Nd)Al_3[(OH)_5(PO_4)_2]\cdot H_2O$

For purposes of this paper, the molecule florencite- (Ce) was considered to be the dominant species, but the entire REE were summed to arrive at the percent florencite molecule in the specimens.

SUMMARY

The specimens from the Bashi Marl of Dale County, Alabama are dominant florencite rather than gorceixite. The Aiken County, South Carolina nodules have a much higher gorceixite content, except for SC 3. It is notable that the SC 3 sample was from the most highly weathered outcrop.

Ariton west, Ariton east and SC 3 all represent nodules from soils overlying the Eocene formations, and all of them are enriched in REE relative to the less weathered samples SC 1 and SC 2. It is interesting to speculate that the REE may be a secondary effect of the nodule weathering; however, as previously noted, the presence of unweathered monazite grains in the nodules argues against such an enrichment. It is possible that the REE enrichment is a localized effect within the formation that the nodules are derived from. Unfortunately, little information on the exact position of the nodules within the enclosing Eocene sediments is available.

Analysis of the unweathered sediments from the level of the crandallite group nodules could shed light on the ultimate source of the Barium, Strontium and REE. Unfortunately, the position of the nodules within the formations has not been determined, nor are cores of the formations available for study.

REFERENCES CITED

Milton, C., J.M. Axelrod, M.K. Carron and F. S. MacNeil. 1958. Gorceixite from Dale County, Alabama. American Mineralogist 43:688-694

Bennett, H. and G.J. Oliver. 1992. XRF analysis of ceramics, minerals and allied materials. John Wiley & Sons, New York.

Michal, J, K.H. Cole and W.S. Moore. 1982. Uraniferous gorceixite in the South Carolina coastal plain (U.S.A.). Chemical Geology. 35:227-245

Szabo, M.W., E.W. Osborne, C.W. Copeland and T.L. Neathery. 1988. Geological Map of Alabama. Geological Survey of Alabama Special Map 220, scale 1:250,000

Dill, H.G., A. Fricke and K.H. Henning.1995. The origin of Ba- and REE-bearing aluminum-phosphate-sulfate minerals from the Lohrheim kaolinitic clay deposit (Rheinisches Schiefergebirge, Germany). Applied Clay Science. 10(3):231-245

Dill, H.G. 2001. The geology of aluminum phosphates and sulfates of the alunite group minerals: A review. Earth Science Reviews. 53(1-2):35-93

Ferguson, R.B., V. Price and W.C. Mosley. 1979. Uraniferous gorceixite occurrences in Aiken County, South Carolina. E.I DuPont de Nemeours and Co., Savannah River Lab (SRL, Aiken S.C. Doc. Ser. DPST-79-318, 19 p.